EVALUATING STABLE CHANNEL ANALYTICAL METHODS FOR DETERMINING STABLE GEOMETRIES IN GRAVEL-BEDDED ALLUVIAL RIVERS

AN ENGINEERING REPORT SUBMITTED IN PARTIAL FULFILLMENT OF THE REQUIREMENTS FOR THE DEGREE OF MASTER OF SCIENCE

Submitted by: William F. Creed
September, 2023
Revised November, 2023

Advisor
Dr. Ryan Morrison
Associate Professor
Civil and Environmental Engineering

WALTER SCOTT, JR
COLLEGE OF ENGINEERING
COLORADO STATE UNIVESRITY

Abstract

The stable channel analytical method is a conceptually-robust, process-driven means of estimating the dimensions of alluvial channels. While it is widely cited in design manuals, few comprehensive studies have been performed evaluating its real-world accuracy. This lack of evaluation is particularly pronounced for gravel-bedded rivers. This is problematic because the analytical method relies heavily on sediment transport equations which are known to have accuracies of +/- 100% to 1,000% in gravel-bedded rivers.

This study tests the accuracy of the stable channel analytical method at 22 sites in the western United States. Design geometries were calculated for each site using numerous method permutations. These geometries were then compared to observed geometries, which are assumed to be quasi-stable. Permutations include different design discharge definitions (effective discharge and half-yield discharge), different sediment transport relations (Meyer Peter-Müller, Einstein-Brown, and Wilcock-Crowe), and different sediment gradations (surface and subsurface).

For most permutations, mean error in design slope was between -3 and 0% of observed slope and mean error in design depth was between -9 and 32% of observed depth. At this accuracy level, the stable channel analytical method is likely suitable for use in river restoration projects. A goal of many river restoration projects is to re-establish a dynamic geomorphic regime which allows for future channel adjustment. This method provides reasonable design geometries from which the river can quickly establish dynamic equilibrium. Engineering applications may require greater accuracy. Result accuracy was found to improve by using the half-yield discharge instead of effective discharge, subsurface gradations instead of surface gradations, and by carefully selecting representative sediment transport equations.

TABLE OF CONTENTS

TABLES

FIGURES

FIGURES (CONT.)

APPENDICES

INTRODUCTION

Channel dimensions are a critical part of any river restoration project. Restoration projects often take place in areas where a channel has been straightened, channelized, or otherwise altered (Soar and Thorne, 2001). In these cases, the designer cannot simply use existing channel dimensions. Existing dimensions are typically unstable, leading either to channel aggradation or degradation. Instead, the designer must calculate stable channel dimensions. At a minimum these include bankfull width, bankfull depth, and longitudinal slope.

Numerous methods have been developed to determine stable channel geometries for alluvial rivers. The earliest of these, the regime method, is predicated on two concepts. First, a single channel forming discharge exists which may be closely approximated as the bankfull discharge (Inglis, 1941; Inglis, 1947). Second, a channel is in dynamic equilibrium when sediment inflow matches sediment outflow at this discharge (Leopold & Maddock, 1953; Hack and Goodlett, 1960). In practice, the equations used in this method were derived for low-gradient, sand bed canals in India and have limited applicability in natural channels (NRCS, 2007).

Hydraulic geometries are another simple method. These are regression equations relating stable channel dimensions to a single variable, bankfull discharge. However, because they make many implicit assumptions about bed material, bank stability, and other factors, they are only applicable to the region for which they were developed (NRCS, 2007). As computing power has increased, numerical sediment transport and geomorphic models have become available. While they directly represent channel forming processes, they are complex and often cumbersome to implement. As a result, their use is limited to large or complex projects (Copeland, 1994).

Analytical methods were developed to fill the gap between simple regime and hydraulic geometry methods and complex numerical models (Copeland, 1994). Analytical methods share three common steps. The first is to identify a single design discharge. The best method of estimating design discharge remains an open area of debate. Most applications of the analytical method use effective discharge, the discharge which transports the most bed material over time (Figure 1; Wolman and Miller, 1960). Other methods of estimating design discharge include flow recurrence intervals (Leopold and Wolman, 1957; Dury, 1973; Hey, 1975), dominant discharge (Blench, 1951), field observations in nearby stable reaches (Williams, 1978), or the half-yield discharge (Scholtes and Bledsoe, 2016). The second step is to

determine the sediment yield from the upstream reach at the design discharge using transport equations. To avoid aggradation or degradation, the sediment transport capacity of the design reach must match the upstream rate of supply (Soar and Thorne, 2001). Finally, continuity equations for flow resistance and sediment transport are solved simultaneously using the design discharge and sediment yield. By constraining two of the three design variables, this returns a family of slope-width or slope-depth relations which satisfy the stability criteria. The third variable may either be picked based on site conditions or constrained using a third equation.

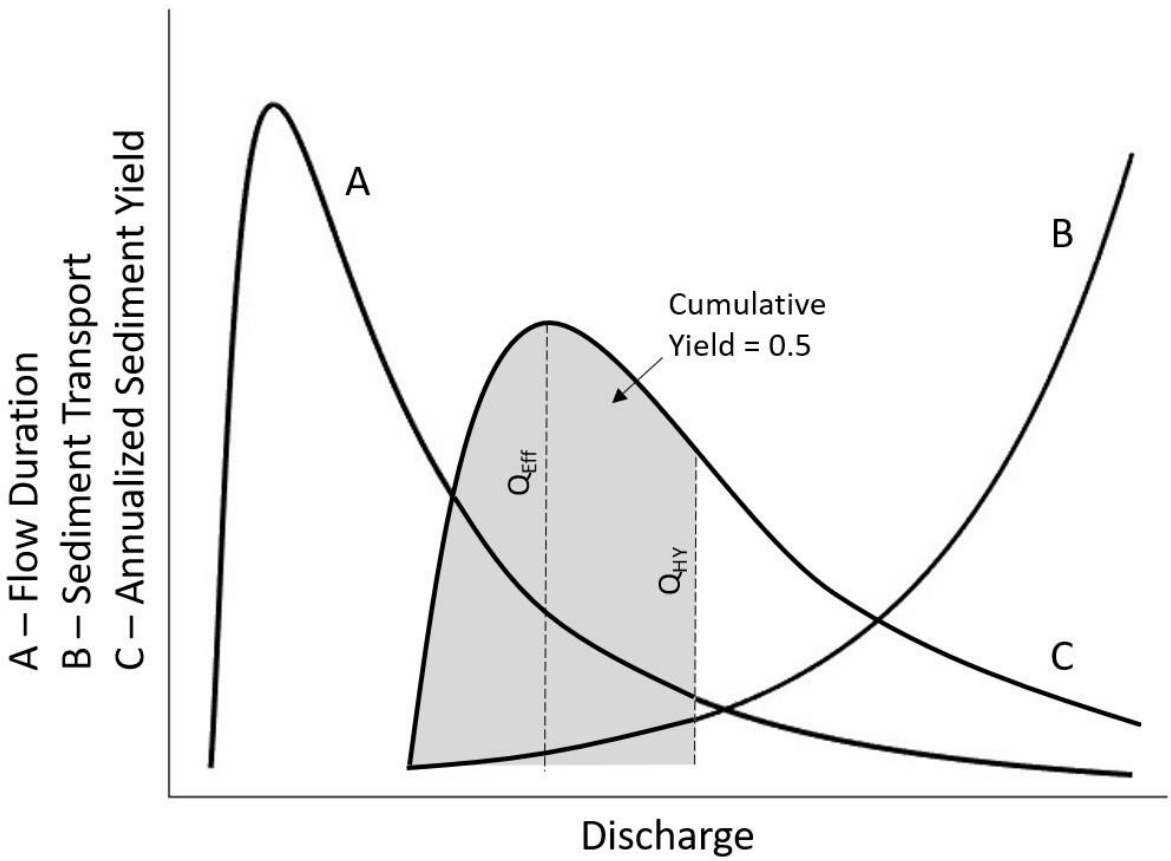

Figure 1: Definitions of effective discharge (Q_{Eff}) and half-yield discharge (Q_{HY})

The first formulation of the analytical method was proposed by Chang, 1980 for use in sand-bed irrigation canals. This method used the Englund-Hansen equations for sediment transport and bedform flow resistance. The third variable was constrained using the minimum stream power equation, an extremal hypothesis. Other early analytical methods were developed by White et al., 1982 and by Abou-Seida and Saleh, 1987. The most commonly applied analytical method was developed by the U.S. Army Corps of Engineers. This method was developed for sand-bed channels and used the

Brownlie equations for sediment transport and bedform flow resistance. Importantly, it partitioned total hydraulic roughness into bed and bank components, allowing for application in hydraulically narrow rivers and channels. It also does not use extremal hypotheses to constrain the third variable (Copeland, 1994). Extremal hypotheses been found to be weak predictors of channel geometry (Griffiths, 1984). More recently, the National Resource Conservation Service (NRCS) has published guidance generalizing the USACE methods to both sand and gravel-bed systems (NRCS, 2007). This generalized method has been further refined to account for multiple design discharges in sand- and gravel-bed rivers by the Capacity-Supply Ratio (CSR) method (Soar and Thorne, 2001; Beldsoe et al., 2017).

All steps in the analytical method rely on sediment transport equations. However, sediment transport equations remain highly inaccurate. The first generation of sediment transport equations were generally able to estimate transport rates within an order of magnitude (Vanoni, 1960). More recent equations are reported to have errors on the order of hundreds of percent (Gomez and Church, 1989; Julien, 2010). However, research has found that transport equations for coarse sediment may still have error on the order of 100% - 1,000% (Habersack and Larrone, 2002; López, Vericat, and Batalla, 2013).

The USACE method acknowledges the limited accuracy of transport equations, focusing on sediment continuity rather than absolute transport rates (Copeland, 1994). However, sediment transport and flow resistance are both non-linear. Even if continuity is maintained, error may still propagate through non-linear equations. No broad evaluation of the accuracy of the USACE stable channel analytical method has been conducted. Evaluation of an earlier version of the analytical method at 213 mostly sand-bedded sites found mean error of 3% for design depth and 102% for design slope (White, Paris, and Bettess, 1981). At this accuracy the stable channel analytical method may have limited applicability in restoration design.

The paucity of large-scale evaluations for the stable channel analytical methods presents a clear research gap. This report evaluates the accuracy of a generalized stable channel analytical method in gravel-bedded rivers. To evaluate accuracy, this method was tested at 22 gravel-bedded alluvial rivers across the western United States.

METHODOLOGY

In order to assess its reliability, the stable channel analytical method was applied to 22 gravel-bedded rivers across the western United States. At each site, stable geometries were calculated using various permutations of equations and inputs. Three different sediment transport equations and two design discharge definitions were used to determine which combination generated the most accurate results. Each combination was evaluated using ranges of observed surface and subsurface sediment gradations. Reliability was assessed based on scatter in predicted geometries and comparison to existing channel geometries, which are presumed stable. Finally, regression analyses were conducted to determine if method reliability can be predicted by geomorphic measurements taken during a standard site assessment.

SITE SELECTION

All data used in this analysis was obtained from previous field studies performed by others. The scientific literature was reviewed to find 49 single-thread, gravel-bedded, alluvial rivers with at least 10 bedload measurements. Bedload measurements are key to evaluating how accurately transport equations estimate bedload transport. Their availability was a limiting factor. Sites meeting these criteria were screened for stability. For channel geometry in sites to be assumed quasi-stable, watersheds with recent wildfires, recent large-scale logging, or large dams were excluded. The effects of historical logging, seismic factors, and other factors acting on a geologic time scale were ignored. Additionally, sites were screened for the availability of sediment gradation data, supporting data for hydraulic calculations, and at least 10 years of daily discharge data.

Twenty-two study sites were identified which meet these criteria. They are located across the western United States in California (Andrews, 1994), Colorado (Ryan et al., 2000; Ryan et al., 2005), Idaho (King et al., 2004; Whiting et al., 1999), and Wyoming (Erwin et al., 2011)(Figure 2). All sites are in semi-arid mountainous regions with snowmelt-dominated hydrographs. Typical of these regions, selected channels are plane-bed or pool-riffle with a mixture of pine trees and willows lining the banks. Settings range from wide open alluvial valleys to narrow semi-confined valleys with floodplain terraces. Bankfull widths at study sites range from 16 to 331 ft. Drainage areas range from 24 to 6,450 mi^2 and bankfull discharges range from 71 to 25,815 cfs (Table 1).

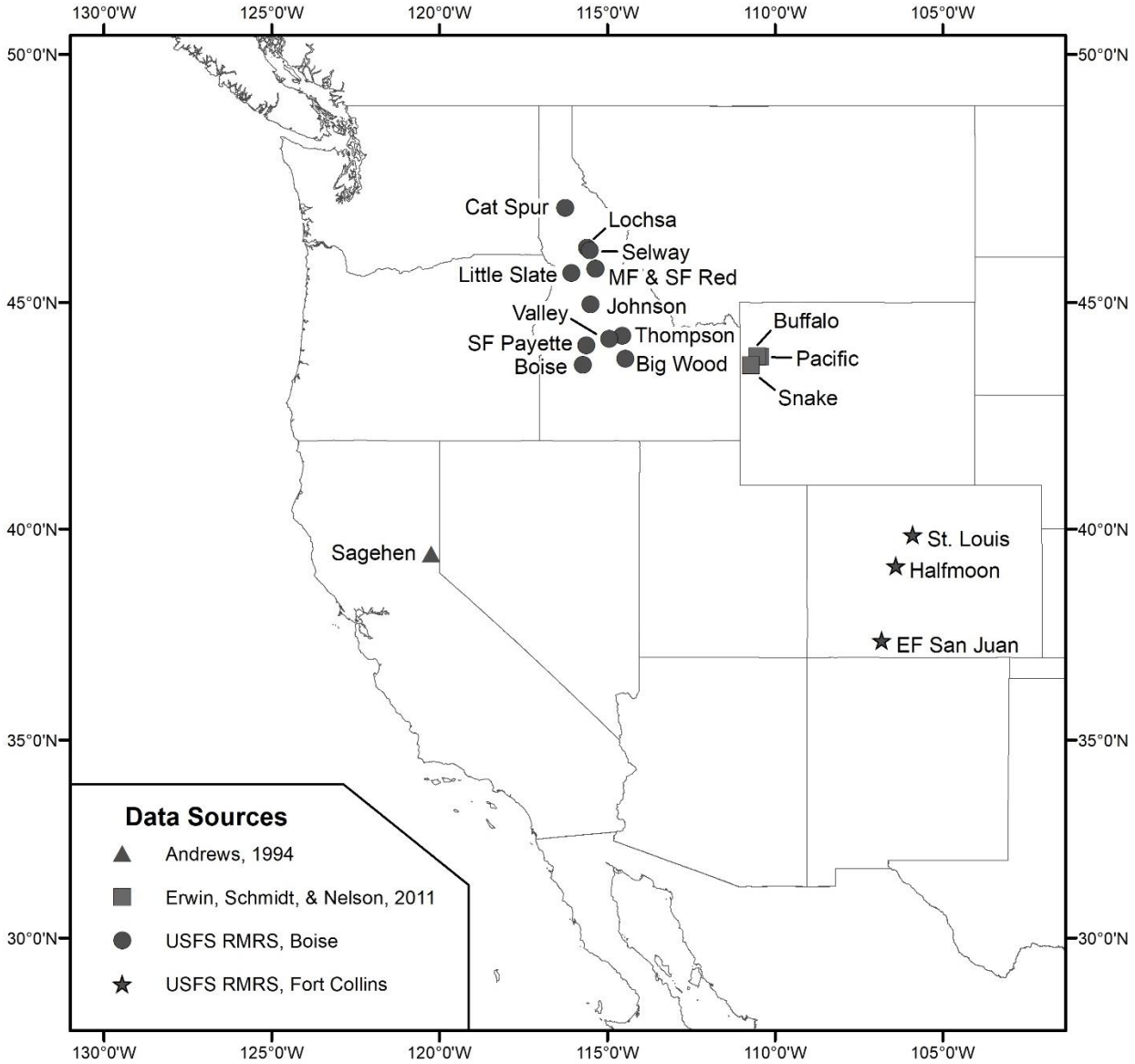

Figure 2: Locations of study sites and sources of field data.

Table 1: Selected characteristics for study sites.

Site	Channel Morphology	Drainage Area (mi^2)	Bankfull Discharge (cfs)	Bankfull Recurrence Interval (yrs)	Bankfull Width (ft)	Bankfull Depth (ft)	Slope (%)	Surface d50 (mm)	Subsurface d50 (mm)	Manning's Roughness, Calibrated	Manning's Roughness, Strickler
Big Wood River, ID	Plane Bed	137	925	2.5	42	3.5	0.91%	169	25	0.04	0.046
Boise River, ID	Riffle	832	6,639	2.0	213	4.8	0.38%	71	22	0.035	0.040
Bufallo Fork, WY	Riffle	323	3,940	1.8	148	4.1	0.25%	19	8.2	0.03	0.032
Cat Spur Creek, ID	Riffle	11.3	83	1.8	16	1.1	1.11%	27	-	0.04	0.034
EF San Juan River, CO	Riffle	64.1	553	1.1	56	1.7	0.80%	23	-	0.025	0.039
Halfmoon Creek, CO	Riffle	23.5	220	1.7	28	1.7	1.50%	64	-	0.035	0.041
Johnson Creek, ID	Plane Bed	218	2,942	1.6	97	7.1	0.40%	79	-	0.045	0.047
Little Slate Creek, ID	Plane Bed	64.6	431	2.0	41	2.1	2.68%	200	-	0.04	0.044
Lochsa River, ID	Riffle	1,178	18,787	2.1	331	10.0	0.23%	122	25	0.04	0.044
MF Red River, ID	Plane Bed	50.2	330	2.0	38	1.8	0.59%	127	27	0.035	0.038
Pacific Creek, wY	Braided Riffle	169	2,600	1.5	141	3.0	0.35%	57	19	0.03	0.033
Sagehen Creek, CA	Riffle	10.5	71	2.0	16	1.3	1.00%	22	15	0.06	0.038
Selway River, ID	Riffle	1,915	25,815	1.7	302	9.9	0.21%	56	30	0.025	0.046
SF Payette River, ID	Riffle	446	4,238	1.9	151	5.1	0.40%	174	25	0.025	0.042
SF Red River, ID	Plane Bed	37.7	256	2.0	36	1.4	1.40%	99	21	0.055	0.042
Snake River, WY	Braided Riffle	6,450	12,400	1.6	230	5.6	0.25%	101	26	0.03	0.036
St. Louis Creek Site 2, CO	Plane Bed	20.9	168	2.3	25	1.4	2.00%	38	25	0.03	0.040
St. Louis Creek Site 3, CO	Riffle	20.8	162	1.3	31	1.2	1.90%	76	-	0.03	0.041
St. Louis Creek Site 4a, CO	Riffle	13.1	127	1.2	23	1.2	2.40%	82	-	0.03	0.042
St. Louis Creek Site 4b, CO	Plane Bed	12.9	119	1.6	27	1.1	2.00%	91	-	0.03	0.042
Thompson Creek, ID	Riffle	29.1	90	1.5	21	1.2	1.53%	79	-	0.025	0.039
Valley Creek, ID	Plane Bed	147	1,010	1.6	105	2.5	0.42%	62	45	0.03	0.038

DATA INTAKE PRIOR TO ANALYSIS

Daily discharge data was accessed for each site from co-located USGS gaging stations or gages established for specific studies. Flow duration curves were generated for periods of record centered on the available bedload measurements. A maximum 30-year period of record was analyzed to avoid potential non-stationarity issues. Additionally, individual water years missing 10% or more of daily data were excluded from the flow duration curve and not included in the period of record length.

Bedload transport rates and sediment gradations were available for all sites. Transport rates were measured using Helley-Smith samplers of varying sizes. Volumetric bedload transport gradations were measured using sieve analyses. Additionally, surface grain size gradations were available for all sites and subsurface grain size distributions were available for most sites. Surface gradations were measured using Wolman pebble counts. Subsurface gradations were measured using sieve analyses. For many sites, gradations were collected at multiple locations and times. To account for this variability, minimum, mean, and maximum gradation curves were developed for sites with multiple measurements.

CHANNEL HYDRAULICS

Stage-discharge relations were developed for each site using stream gaging records and normal depth calculations. Normal depth calculations use surveyed cross-sections, slopes from the primary studies, and a single Manning's roughness coefficient for the entire channel width (Table 1). This roughness coefficient was calibrated based on stream gaging records. Calibration focused on higher discharges comparable to the bankfull and effective discharges. Calibrated roughness coefficients were comparable to grain roughness estimated from the Strickler Equation (Eq. 1)

$$n = 0.064 d_{50}^{\frac{1}{6}} \tag{1}$$

Where n is the Manning's roughness coefficient and d_{50} is the median particle diameter in meters.

The closeness of total roughness to grain roughness values from the Strickler equation indicate that the effects of vegetation or bedforms are negligible for in-channel hydraulics. Therefore, shear stresses were not partitioned into grain and from components. Shear stress-discharge relations were developed using the depth-slope product (Eq. 2)

$$\tau = \gamma R_h S \tag{2}$$

Where τ is shear stress, γ is specific weight, R_h is hydraulic radius, and S is longitudinal slope.

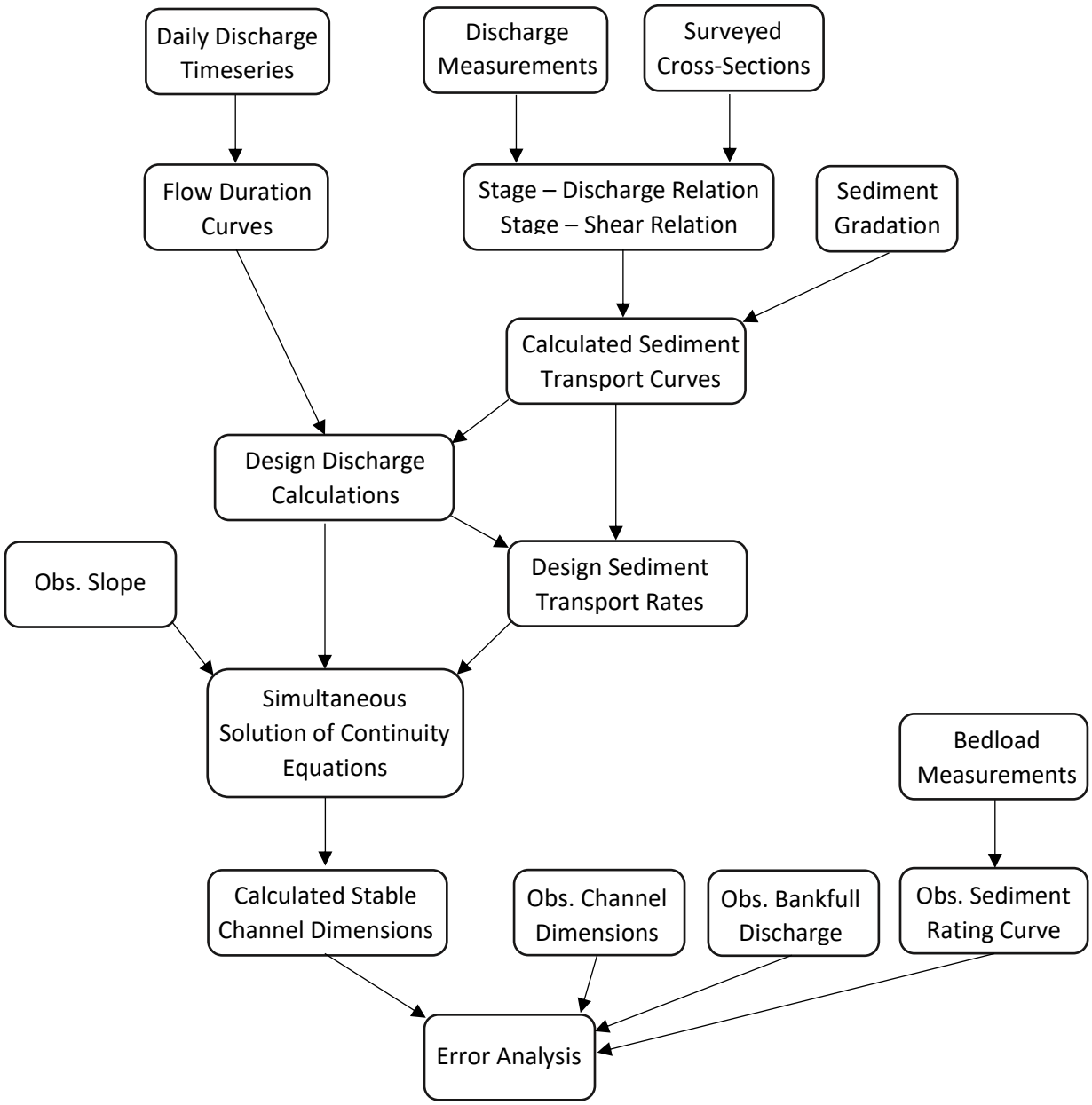

Figure 3: Generalized analysis workflow.

SEDIMENT RATING CURVES

Bedload rating curves were developed from observed bedload measurements. These rating curves were fit using single-piece power functions and incorporate best-practices from the USACE and the U.S. Geological Survey (USGS)(Gray and Simoes, 2008; Gibson, 2021). Based on these recommendations, the Duan smearing factor was used to remove statistical bias introduced by fitting curves to logarithmically transformed data. Additionally, bedload measurements collected at discharges equal to the 50% exceedance flow or lower were excluded. For almost all sites, bedload measurements were only collected over a 2 – 5 year period. Given this short period of record, stationarity analyses were not performed.

$$Q_{bv} = c_{duan}\alpha Q^{\beta} \tag{3}$$

Where:

Q_{bv} = volumetric bedload transport
Q = river discharge
α & β = dimensionless regression coefficients
c_{duan} = dimensionless Duan smearing factor (Duan, 1983).

Sediment transport curves were also estimated using three bedload transport equations: Meyer-Peter-Muller, Einstein-Brown, and Wilcock-Crowe. These equations were selected based on their wide application in the United States and because each represents sediment transport using different principles. A fourth equation, the Parker-Klingeman equation (Parker and Klingeman, 1982), was not used because bed material for several sites had significant sand fractions. Note that for many sites the median particle diameter exceed the size particles used to derive available transport equations.

The Meyer Peter-Müller equation determines bedload transport as a function of excess shear stress. It was derived from flume experiments with gravel sized particles ranging from 4.3 to 30 mm (Meyer-Peter and Müller, 1948). As such, it is applicable to gravel-bedded channels where suspended load is minimal (Chang, 1998). The original equation was simplified by Chien, 1956 to

$$q_{bv} = 8\sqrt{(G-1)gd_s^3}(\tau_* - T_{c*})^{3/2} \tag{4}$$

Where:

q_{bv} = volumetric sediment transport per unit width
G = specific gravity of sediment
g = gravimetric acceleration
τ_* = dimensionless shear stress
τ_{*c} = critical Shields parameter (0.047 when using Meyer Peter-Müller equation)

The Einstein-Brown equation determines bedload transport using a probabilistic model based on dimensionless shear stress (Einstein, 1942; Einstein, 1950). Unlike the Meyer Peter-Müller equation, sediment transport is predicted at all discharges. Modifications to the original equations by Brown, 1950 yield the Einstein-Brown equations

$$q_{bv^*} = \begin{cases} 2.15e^{-\frac{0.391}{\tau_*}}, & \tau_* < 0.18 \\ 40\tau_*^3, & 0.18 < \tau_* < 0.52 \\ 15\tau_*^{1.5}, & \tau_* > 0.52 \end{cases} \tag{5a}$$

where q_{bv^*} is the dimensionless volumetric sediment transport rate per unit width and τ_* is dimensionless shear stress. Sediment transport rates may be dimensionalized using

$$q_{bv} = \omega_0 d_s q_{bv^*} \tag{5b}$$

where ω_0 is particle settling velocity and d_s is median particle diameter. For this study, both the Meyer Peter-Müller and Einstein-Brown equations were evaluated using median (D_{50}) particle diameters from each gradation.

The Wilcock-Crowe equation (Wilcock and Crowe, 2003), a common method that directly represents multiple sediment gradations and the sand fraction, is defined as

$$W_i^* = \begin{cases} 0.002\phi^{\frac{15}{2}}, & \varphi < 1.35 \\ 14\left(1 - \frac{0.894}{\phi^{\frac{1}{2}}}\right), & \varphi \geq 1.35 \end{cases} \tag{6a}$$

Where W_i^* is the dimensionless bed load transport parameter for the ith particle size fraction and ϕ is the ratio of the shear stress acting on the bed surface (τ_i) to the reference shear stress for the ith size fraction (τ_{ri}). Bedload transport may be dimensionalized by

$$W_i^* = \frac{(s-1)gq_{bi}}{F_i u_*^3} \tag{6b}$$

where *s* is the specific gravity of sediment, *g* is gravimetric acceleration, q_{bi} is volumetric sediment transport per unit width for the ith particle size fraction, F_i is fraction of the bed surface consisting of the ith size fraction, and u_* is shear velocity.

Dimensionless reference shear stress is is analogous to the critical Shields number used in earlier methods. It is defined as the shear stress which at which W_i^* = 0.02, and may be calculated for the median diameter surface particle size using

$$\tau_{rm}^* = 0.021 + 0.015e^{-20F_s} \tag{6c}$$

where τ_{rm}^* is the dimensionless reference shear stress for the median surface particle and F_s is the sand fraction of the surface material. This may be dimensionalized using

$$\tau_{rm} = \tau_{rm}^*(s-1)\rho g D_{sm} \tag{6d}$$

where ρ is the density of water and D_{sm} is the grain diameter of the median surface particle. Reference shear stresses for all other surface size fractions may then be calculated as

$$\frac{\tau_{ri}}{\tau_{rm}} = \left(\frac{D_i}{D_{sm}}\right)^b \tag{6e}$$

where D_i is the grain diameter of the ith size fraction and *b* is an empirically fit coefficient defined as

$$b = \frac{0.67}{1 + e^{\left(1.5 - \frac{D_i}{D_{sm}}\right)}} \tag{6f}$$

STABLE GEOMETRY CALCULATIONS

Stable geometries were calculated using methodology presented in the NRCS National Engineering Handbook Part 654.9 (NRCS, 2007) which presents a more generalized form of the analytical method than the USACE. Numerous permutations of this model were tested using different design discharge definitions, sediment transport equations, and sediment gradations. Thirteen combinations of sediment transport equations and sediment gradations were considered for each site (Table 2). Each of these combinations was evaluated using three definitions of design discharge: effective discharge, half-yield discharge, and observed bankfull discharge. Evaluating combinations with both effective and half-yield discharges allows an assessment of the relative accuracies of both definitions. Evaluating combinations using bankfull discharge removes error from the first two steps, isolating error in the final simultaneous solution. For the remainder of this report pairs of sediment transport equations, sediment gradations, and design discharge definitions are referred to as method permutations.

Table 2: Combinations of sediment transport equation and sediment gradation used in analysis for each site.

		Sediment Transport Equation		
		Meyer Peter-Müller	Einstein-Brown	Wilcock-Crowe
Surface Gradation	Min.	X	X	-
	Mean	X	X	X
	Max.	X	X	-
Subsurface Gradation	Min.	X	X	-
	Mean	X	X	-
	Max.	X	X	-

The first step in the stable channel analytical method is to calculate design discharge. Effective discharges were calculated using methodology from Biedenharn et al., 2000. For each site the daily flow record was divided into 15 to 25 arithmetic bins. For each combination in Table 2, bedload transport rates were calculated for mean bin discharges. Transport rates were multiplied by annual bin frequency to determine the annualized sediment transport rates. Effective discharge was then calculated as the mean flow for the bin with the highest annualized sediment transport rate (Figure 4a).

Definite rules have not been developed for the number of bins (Biedenharn et al., 2000). Hey, 1997 recommends that 10 – 25 arithmetic bins be used in most cases while Yevjevich, 1972 recommends that bin widths be less than one quarter the standard deviation of daily flow data. This guidance proved conflicting for many sites. Where results were not affected by discontinuities in the flow duration cure, 25 bins were used. Where effective discharge was identified in a bin adjacent to a bin with zero flow probability, the number of bins was reduced. For most sites effective discharge was not sensitive to the number of bins.

Annualized sediment transport rates were also used to calculate the half-yield discharge. Annual sediment transport rates from each bin were integrated to form a cumulative density function (CDF) of annualized transport rates. The half yield discharge was calculated as the flow corresponding to the 50th percentile from the CDF for each combination at each site. Bankfull discharge were obtained from reported values from primary studies.

The second step was to determine the design sediment yield. For the design discharge from each method permutation, sediment transport rates were calculated using the corresponding sediment transport equation and sediment gradation.

The final step was to calculate stable channel geometries that provide continuity for the design discharge and sediment yield. Stable geometries were calculated using hydraulic resistance and sediment transport as the first two constraints. Bankfull width was selected as the third constraint. This was set as the observed bankfull width, which was assumed to be stable. Using these constrains, stable depth-slope pairs were calculated for each method permutation. Based on availability, up to 27 depth-slope pairs were calculated for each site (Figure 4b). Of these, 13 used effective discharge and 13 used half-yield discharge. When evaluated using bankfull discharge, all combinations of sediment transport equation and gradation returned the same depth-slope pair. Depth slope pairs were not calculated for model permutations at individual sites with very low sediment transport rates (< 1g/s).

In these cases, the need to provide hydraulic continuity with negligible sediment transport resulted in geometries which would be obviously incorrect to the average practitioner.

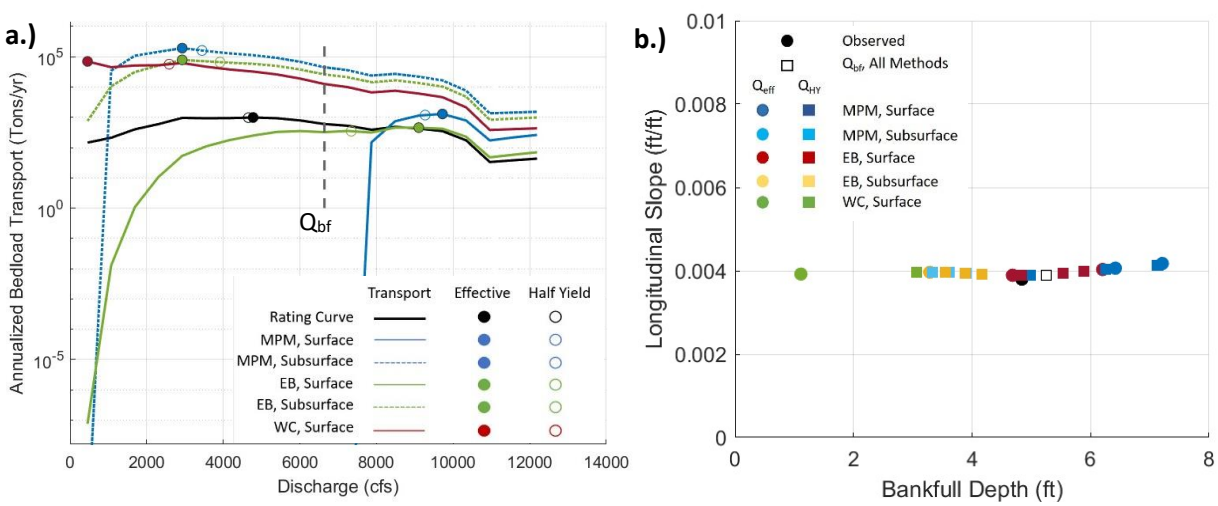

Figure 4: Example outputs for the Boise River, ID showing a.) effective discharge and half-yield discharge calculations, and b.) stable geometry outputs for each permutation of transport equation, design discharge method, and sediment gradation.

ERROR ANALYSIS

The overall reliability of the stable channel analytical method was assessed by quantifying error in four parameters. The primary focus was on depth and slope outputs, but design discharge and design sediment load, two key intermediate parameters, were also considered. Error was calculated relative to observed conditions. Observed slope, bankfull depth, and bankfull discharge were obtained from prior studies. Observed bankfull sediment load was calculated from sediment rating curves. To compare results between sites, error was normalized and expressed as the percent difference between computed and observed values.

Error was analyzed in two ways. First, summary statistics were calculated separately for each method permutation. These include mean and standard error as well as the probability that error falls within acceptable ranges. Given the small number of data points available for some permutations, probabilities were calculated from empirical cumulative density functions not fitted distributions. These statistics were used to determine overall method accuracy as well as the relative accuracy of individual method permutations.

Correlation of error was also considered. Regression analyses were performed between two sets of parameters. To determine how error propagates through calculations, error in intermediate design parameters was related to error in final design geometries. To determine if a prior estimates of design accuracy can be made for an individual site, field measurements were related to error in design geometry. Field measurements were limited to parameters which design engineers may have access to on a typical project. These include basic hydrologic data, longitudinal slope, and sediment gradation parameters.

Note that this analysis assumes that channel dimensions at all sites are quasi-stable. If channel dimensions are not quasi-stable due to land use change, climate change, the presence of bedrock sills, or other factors, mean error will be incorrect but standard error will still be accurate. Standard error is a useful indicator of how reliable method results are given variations in user assumptions and inputs.

RESULTS

GENERAL RESULTS

Error in the stable channel analog method begins with error in sediment transport equations. At bankfull discharges, error in bedload from the three sediment transport equations used in this study ranged from -97% to 25,000% or more. In 10% of cases bedload transport was overestimated by at least 100,000%. Additionally, transport equations for many sites did not reflect the shape of observed sediment transport rating curves. The Meyer Peter-Müller and Einstein-Brown equations tended to overpredict the slope of the rating curve when using surface gradations. Conversely, they tended to match or underpredict the slope of the rating curve when using subsurface gradations. The Wilcox Crowe equation generally matched or underpredicted slope of the bedload rating curve.

Error in the shape of computed transport relations effected the accuracy of effective discharge and half-yield discharge calculations (Schulte, 2014). Permutations using surface gradations, which overestimate the slope of the transport curve, also overestimated design discharges by an average of 40 to 60% (Table 3; Figure 5). Permutations that used subsurface gradations or the Wilcox Crowe equation, which typically matched or underestimated the slope of the transport curve, tended to underestimate design discharge. These permutations were more accurate with mean error between -20 and -40%. These trends held for both the effective discharge and half-yield discharge definitions (Table 4; Figure 6).

Error in both the magnitude of computed sediment transport rates and the design discharge effected the accuracy of design geometries. On average, permutations using surface gradations overestimated stable depths by 13 to 32%. In contrast, permutations using sub-surface gradations underestimated stable depths by 9 to 20%. Standard error was on the order of 30 to 40% for all permutations (Table 5; Figure 7). Computed depths were within +/-50% of observed depths for 74 – 90% of sites for all permutations except those using the Wilcock-Crowe equation (Table 7). In contrast, computed design slopes closely matched observed slopes for all method permutations. Mean error in slope was between -3% and 0% for all permutations, and standard error was on the order of 10% to 20% (Table 6; Figure 8). Computed slopes were within +/-25% of observed slopes for 87 - 94% of sites and within +/-10% of observed slopes for 57 - 75% for of sites (Table 8).

Table 3: Summary statistics of normalized error in design discharge for selected method permutations.

	Effective Discharge			Half Yield Discharge		
	Mean	Median	SD	Mean	Median	SD
Rating Curve (n = 22)	11%	-9%	69%	5%	-19%	54%
Meyer-Peter Muller, Surface Gradation (n = 22)	46%	47%	104%	61%	48%	90%
Meyer-Peter Muller, Subsurface Gradation (n = 14)	-42%	-47%	29%	-33%	-43%	23%
Einstein-Brown, Surface Gradation (n = 22)	52%	41%	53%	43%	27%	53%
Einstein-Brown, Subsurface Gradation (n = 14)	-22%	-35%	36%	-19%	-29%	30%
Wilcock - Crowe (n = 22)	-53%	-65%	49%	-17%	-34%	44%

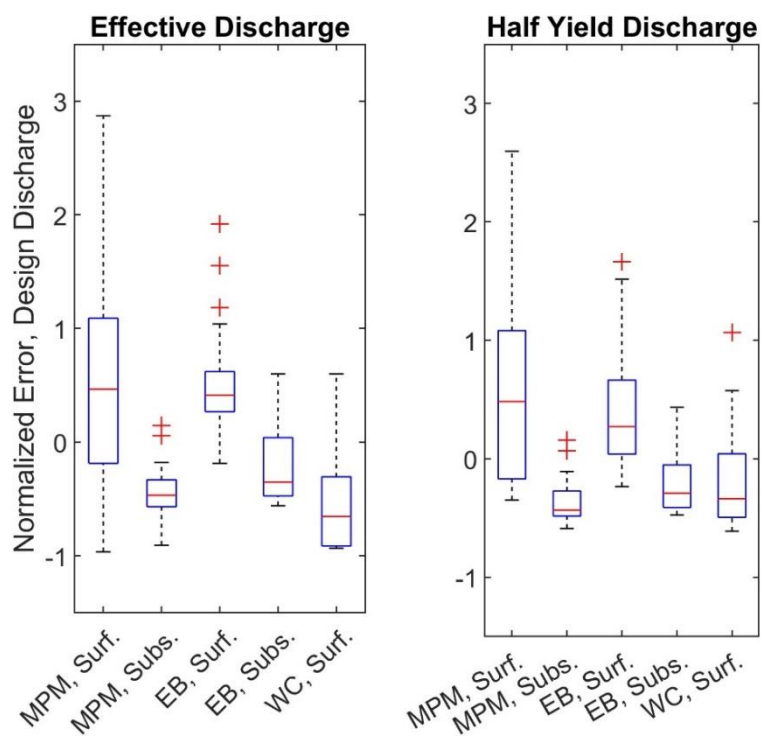

Figure 5: Distributions of normalized error in design discharge for selected method permutations. Boxplot shows quartiles and statistical outliers.

Table 4: Summary statistics of normalized error in design sediment load for selected method permutations.

	Effective Discharge			Half Yield Discharge		
	Mean	Median	SD	Mean	Median	SD
Rating Curve (n = 22)	256%	-16%	494%	134%	-45%	283%
Meyer-Peter Muller, Surface Gradation (n = 22)	5094%	1341%	7417%	5902%	1367%	8473%
Meyer-Peter Muller, Subsurface Gradation (n = 14)	13503%	5767%	18866%	11371%	3385%	16706%
Einstein-Brown, Surface Gradation (n = 22)	1932%	302%	4290%	1285%	141%	2100%
Einstein-Brown, Subsurface Gradation (n = 14)	6647%	1465%	10514%	6994%	1862%	11391%
Wilcock - Crowe (n = 22)	206%	30%	674%	1174%	254%	1779%

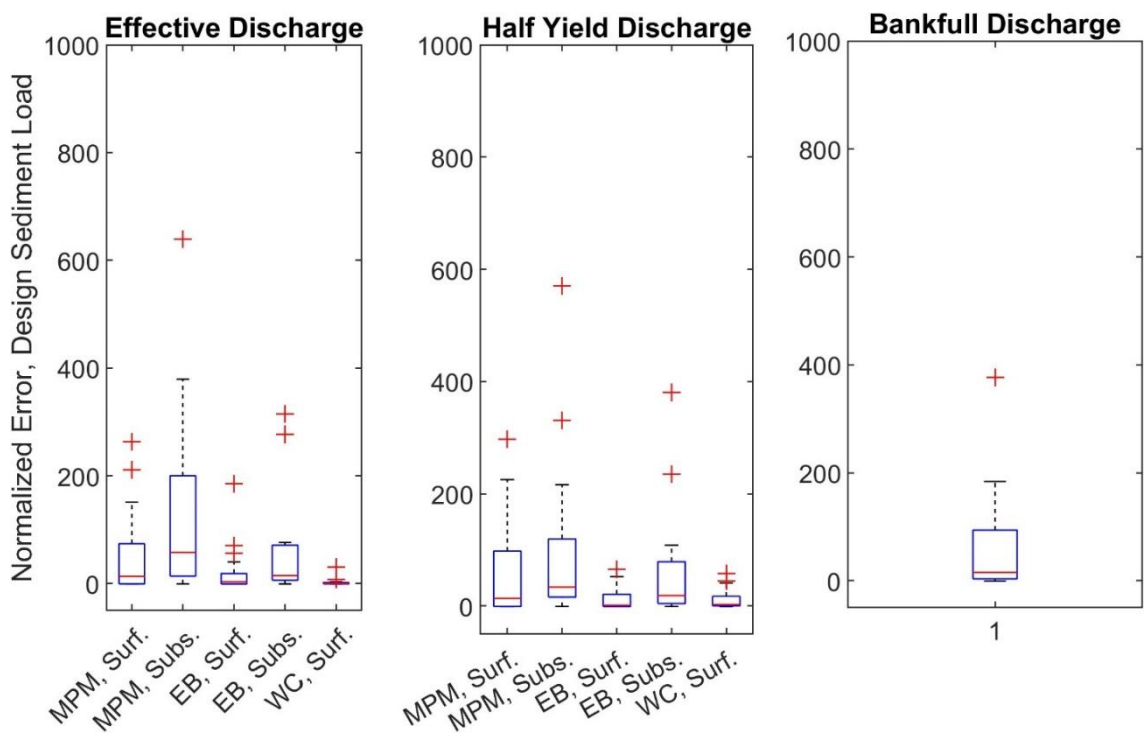

Figure 6: Distributions of normalized error in design sediment load for selected method permutations. Boxplot shows quartiles and statistical outliers.

Table 5: Summary statistics of normalized error in design depths for selected method permutations.

	Effective Discharge			Half Yield Discharge		
	Mean	Median	SD	Mean	Median	SD
Meyer-Peter Muller, Surface Gradation (n = 22)	32%	28%	38%	22%	13%	29%
Meyer-Peter Muller, Subsurface Gradation (n = 14)	-20%	-25%	35%	-13%	-21%	30%
Einstein-Brown, Surface Gradation (n = 22)	21%	15%	27%	13%	12%	23%
Einstein-Brown, Subsurface Gradation (n = 14)	-12%	-19%	32%	-9%	-17%	28%
Wilcock - Crowe (n = 22)	-37%	-46%	46%	-13%	-14%	31%

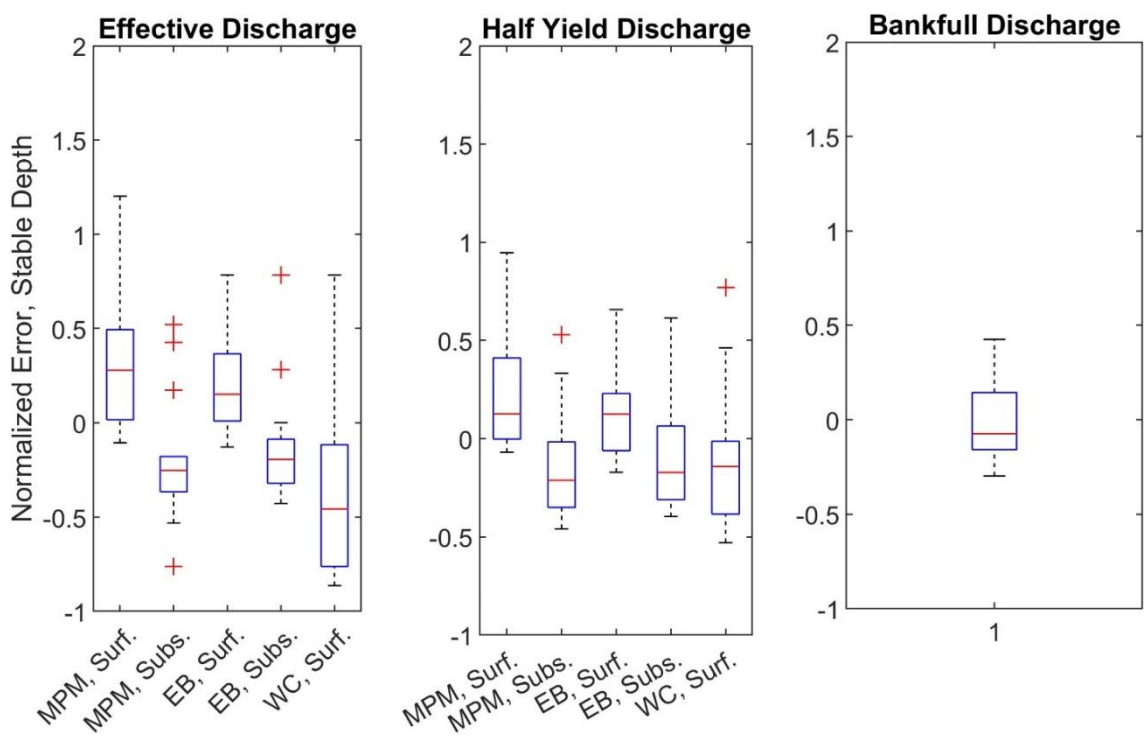

Figure 7: Distributions of normalized error in design depths for selected method permutations. Boxplot shows quartiles and statistical outliers.

Table 6: Summary statistics of normalized error in design slopes for selected method permutations.

	Effective Discharge			Half Yield Discharge		
	Mean	Median	SD	Mean	Median	SD
Meyer-Peter Muller, Surface Gradation (n = 22)	2%	0%	13%	-7%	-3%	35%
Meyer-Peter Muller, Subsurface Gradation (n = 14)	-2%	-2%	9%	-3%	-2%	10%
Einstein-Brown, Surface Gradation (n = 22)	8%	0%	26%	1%	-1%	12%
Einstein-Brown, Subsurface Gradation (n = 14)	-1.19E-05	-1%	11%	-2%	-2%	9%
Wilcock - Crowe (n = 22)	2%	0%	15%	1%	-1%	9%

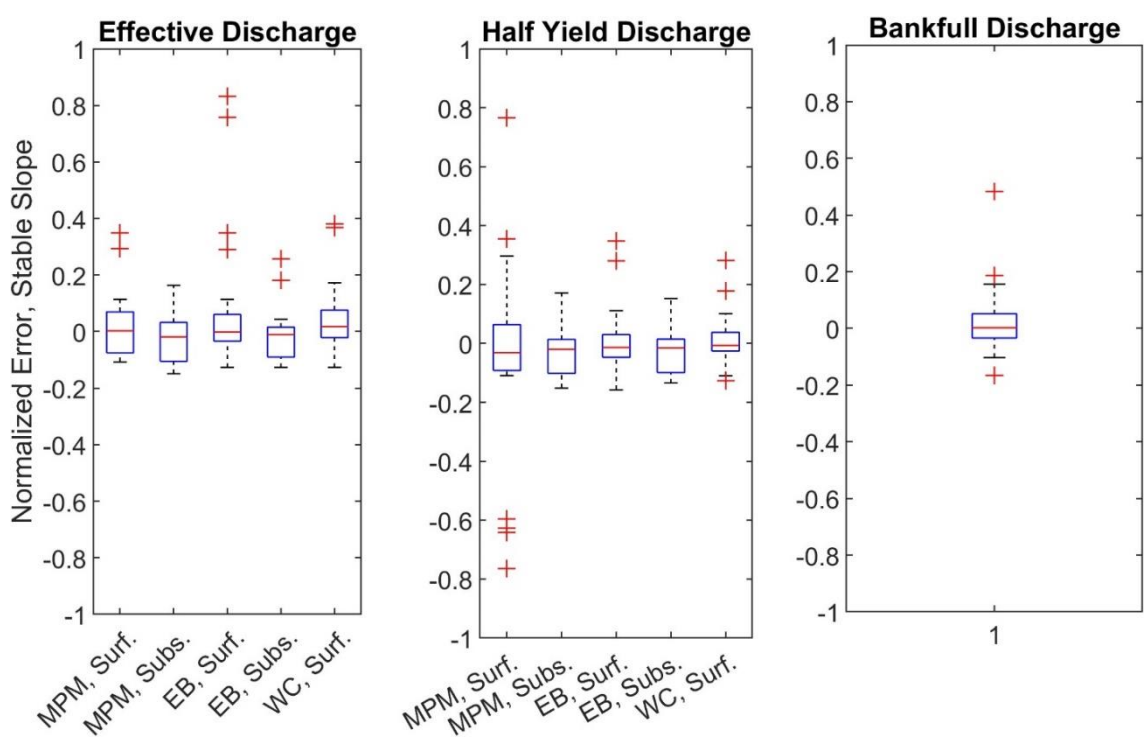

Figure 8: Distributions of normalized error in design slopes for selected method permutations. Boxplot shows quartiles and statistical outliers.

Table 7: Percentage of sites with design depths within specified normalized error ranges. Percentages calculated using Weibull plotting position.

	Effective Discharge					Half-Yield Discharge				
	MPM		EB		WC	MPM		EB		WC
Normalized Error	Surf, Mean	Subs, Mean	Surf, Mean	Subs, Mean	Surf, Mean	Surf, Mean	Subs, Mean	Surf, Mean	Subs, Mean	Surf, Mean
+/- 10%	28%	4%	32%	19%	12%	35%	15%	26%	23%	19%
+/- 20%	40%	14%	50%	35%	18%	42%	28%	65%	45%	49%
+/- 30%	51%	43%	68%	53%	24%	55%	49%	76%	54%	53%
+/- 40%	70%	60%	73%	78%	34%	63%	69%	85%	89%	72%
+/-50%	74%	76%	78%	90%	46%	74%	92%	88%	91%	86%
+/- 100%	90%	93%	95%	93%	96%	90%	93%	95%	93%	96%

Table 8: Percentage of sites with design slopes within specified normalized error ranges. Percentages calculated using Weibull plotting position.

	Effective Discharge					Half-Yield Discharge				
	MPM		EB		WC	MPM		EB		WC
Normalized Error	Surf, Mean	Subs, Mean	Surf, Mean	Subs, Mean	Surf, Mean	Surf, Mean	Subs, Mean	Surf, Mean	Subs, Mean	Surf, Mean
+/- 10%	71%	57%	59%	61%	64%	73%	56%	71%	57%	75%
+/- 20%	86%	93%	79%	87%	88%	86%	93%	88%	93%	92%
+/- 25%	88%	93%	80%	92%	89%	87%	93%	89%	93%	94%
+/- 30%	90%	93%	82%	93%	90%	89%	93%	91%	93%	96%
+/- 40%	94%	93%	87%	93%	96%	94%	93%	95%	93%	96%

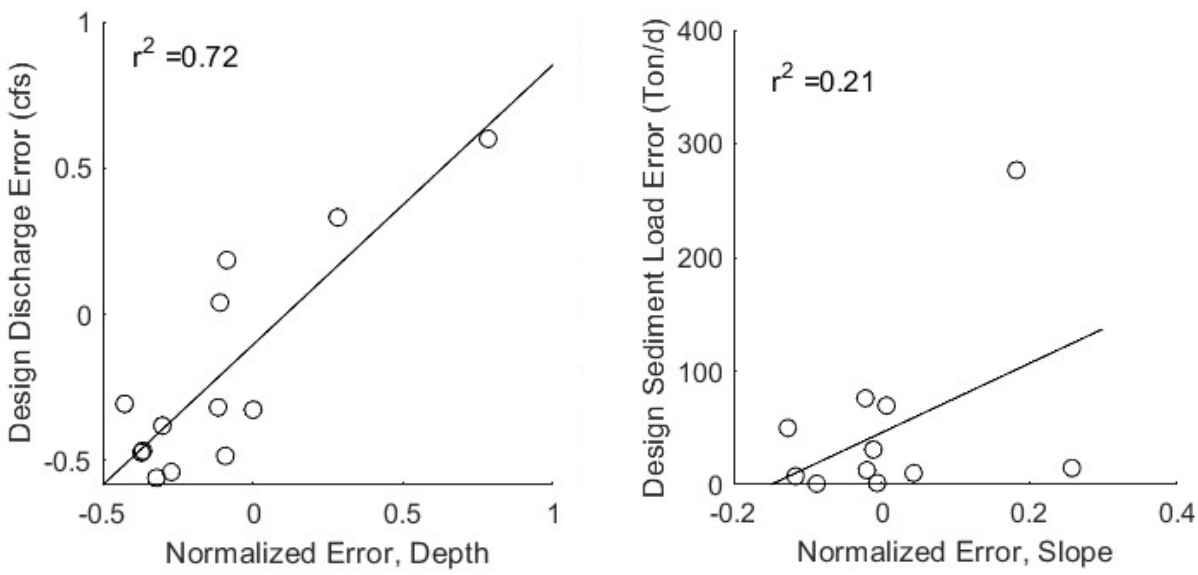

Figure 9: Simple linear regression between error in intermediate parameters and resulting geometries using the Einstein-Brown equation, median subsurface gradation, and effective discharge. Results are illustrative of all method permutations.

REGRESSION ANALYSES

Regression analysis showed that error in design depth was strongly correlated with error in design discharge (Figure 9a). Depending on method permutation, the coefficient of determination between the two ranged from 58 - 83%. Error in slope was not correlated with error in design discharge, but was weekly correlated with error in design sediment load (Figure 9b). However, four sites had far greater error in design slope than the other 19 sites. These sites tended to have lower discharges, steeper longitudinal slopes, and lower bankfull bedload transport rates than sites where bankfull discharge was accurately estimated.

While error in stable geometries could be predicted from intermediate parameters, it could not be predicted from readily observed field measurements. Of the nine field measurements analyzed, only three were found to have moderate statistical correlation for certain permutations. The subsurface gradation coefficient was found to be a weak predictor of error in design discharge for three of five primary permutations (i.e., excluding permutations with minimum or maximum sediment gradations; r^2 = 0.31 to 0.55). Longitudinal slope was found to be a moderately strong predictor of error in design discharge for two of five primary permutations (r^2 = 0.41 to 0.67). Armoring ratio was found to be a weak predictor of error in design depth for two of five primary permutations (r^2 = 0.31 to 0.34). No statistically significant predictor was found for error in design slope and no statistically significant predictor found for all method permutations. See figures in Appendix B.

BANKFULL DISCHARGE ANALYSIS

A more nuanced understanding of error was made by comparing results from permutations using calculated design discharges (i.e., effective or half-yield) to permutations using observed bankfull discharge. Assuming observed channel dimensions are stable, starting with observed bankfull discharge removed error from design discharge calculations. This allowed for a quantification of where error was introduced in the analytical method: either from the design discharge calculations, from the simultaneous solution of transport equations, or from parameters not represented in the method.

When starting from observed bankfull discharge, mean error for depth was -1% and median error for slope was 2%. However, all results were not this accurate. Normalized error in depth had a standard deviation of 20% and normalized error in slope had a standardized deviation of 13% (Figures 7 & 8). This error likely came from the simultaneous solution of transport equations. It may also have come from factors not represented in the method such as riparian vegetation. By comparison, method

permutations using calculated discharge typically had a 10 – 20% error in mean depth. Scatter in the error of both design depth and slope was doubled when calculating design discharge.

METHOD PERMUTATIONS

Different method permutations had different accuracies. The most significant difference in accuracy was between permutations using effective and half-yield discharges. Regardless of which sediment transport relation was used, permutations using the half-yield discharge estimated design discharge 20 to 60% more accurately than permutations using the effective discharge (Table 3; Figure 5). For computed depths, this translated into a 30% reduction in mean error and a 10 – 20% reduction in standard deviation (Table 5; Figure 7). No significant differences were observed between design sediment loads and slope computed using the half-yield discharge versus the effective discharge (Tables 4 & 6; Figures 6 & 8).

Selection of transport equation also had important implications for method accuracy. Both the Meyer Peter-Müller and Einstein-Brown equations had similar mean error for design discharge, but standard deviations for the Einstein-Brown method were approximately 50% lower (Table 3; Figure 5). This translated into 30 to 40% lower mean error in design depth for the Einstein-Brown equation versus the Meyer Peter-Müller equations (Table 5; Figure 7). This result was independent of gradation source or design discharge definition. The Einstein-Brown equations also had significantly less error in design sediment yield, but this did not translate into less error in design slopes (Tables 4 & 6; Figures 6 & 8). While the Wilcox-Crowe equation frequently provided the best match to the observed sediment rating curve, it had amongst the highest error in design discharge and design depth.

For sites where multiple sediment gradations were available, use of minimum, mean, or maximum gradation impacted accuracy. While the small number of sites with multiple gradations, especially subsurface gradations, precluded a rigorous statistical analysis, general patterns could still be established. Use of maximum gradations was found to steepen sediment transport relations, resulting in higher design discharges. For permutations using surface gradations this translated into increased depths and scatter in depths. Increases were also observed for subsurface permutations, but these changes were secondary to changes from design discharge and transport equation. Increases in sediment gradation resulted in an obvious decrease in design sediment loads. Decreases in sediment load had minimal effects on slope for permutations using subsurface gradations but led to increased error when using surface gradations.

DISCUSSION

Despite error in calculated sediment transport rates on the order of 1,000% to 100,000% for many test sites, the stable channel analytical method was found to be an accurate predictor of channel geometries. It is best at predicting slope. Median error for all permutations was 3% or less for all sites and standard error was on the order of 10 to 20%. It is also a robust predictor of depth. When using subsurface-based methods, mean error was on the between -9 and 32%. For a large river this may cause the design depth to be off by several feet. For a small creek, the design depth may be off by several inches. While depths from individual method permutations contained significant error, comparison of depths from multiple permutations or from other methods should give accurate estimate of stable depth. Method accuracy was found to improve by using the half-yield discharge instead of design discharge, subsurface gradations instead of surface gradations, and by carefully selecting representative sediment transport equations.

Compared to comparable methods, the stable channel analytical method is a reliable estimator of bankfull geometries in gravel-bedded rivers. For gravel-bedded rivers, regime equations have a mean error of 160% and standard error of 430% (Griffiths, 1981). Traditional hydraulic geometry relations developed for gravel bedded rivers typically have mean average errors of 10% in depth and 20% in slope (Gholami et al., 2019a), but with higher standard deviations in error than the stable channel analytical method. Only more recent hydraulic geometry relations developed with machine learning techniques have higher accuracies than the stable channel analytical method. Relations for arid, gravel-bedded rivers have mean average errors as low as 4% (Gholami, et al., 2019b) and relations for humid sand-bed river have mean average errors as low as 12% (Harun et al., 2021). However, these empirical equations lack the broader applicability of the stable channel analytical method.

Simplifications in the experimental setup may limit the broader applicability of these findings. All sites used in this study are from semi-arid regions of the western United States. The applicability of the design discharge concept as well as the appropriateness of specific definitions used to calculate design discharge are known to vary with climate (Andrews, 1980; Doyle et al., 2007). Including sites from other climates such as the Pacific Northwest or Appalachian Mountains may change conclusions about the accuracy of design discharge methods, and therefore the accuracy of design depths. Additionally, all calculations are based on simplified 1D hydraulics. Accounting for cross-sectional variability in shear stress and particle diameter typically results in greater sediment mobility (Ferguson, 2003; Monsalve et

al., 2020). Representing cross-sectional variability may improve estimates of design sediment load and stable slope, particularly when using excess shear methods such as the Meyer Peter-Müller equation.

Additionally, this study only included a statistical analysis of how error propagates through the method, not a mechanistic or mathematic understanding of the sources of error. A more rigorous analysis could shed light on why design slopes and the half-yield discharge are more accurate, as well as other outstanding issues. Using previous studies and regression analysis performed as part of this study, inferences can still be made about some of these issues. Sholtes et al., 2016 shows that half-yield discharge is a better predictor of bankfull discharge than effective discharge, particularly systems with coarse bed materials. All systems used in this analysis have coarse bed material. Another issue is the form of the Meyer-Peter Muller equation. This study used the original equation as simplified by Chien, 1956. Wong and Parker, 2005 revised the equation and showed that the original form overestimated transport by a factor of 2.0 to 2.5. Because the revised equation is a linearly-scaled version or the original, its use would only change design sediment load, not design discharge. Design depth was found to be insensitive to error in design sediment load. Design slope was found to be moderately sensitive to error in design sediment load, but typically when error was on the order of one or more orders of magnitude. Decreasing the design sediment load by a factor of two likely would not significantly change estimates of slope, which were generally accurate even with large errors in design sediment yield.

There are several important factors which the stable channel analytical method does not incorporate. Chanel-forming discharge calculations, on which the stable channel analytical method is based, are frequently criticized for focusing on a single discharge. While use of a single discharge is a convenient simplification, research has repeatedly found restoration designs should consider a range of flows (Costa and O'Connor, 1995; Davidson and Eaton, 2018). Research conducted since the analytical methods were originally developed highlights the importance of riparian vegetation and large wood on channel morphology (Schum, 1981; Beechie et al., 2006; Wohl et al., 2019). Additionally, this method does not account for limitations in sediment supply.

Finally, it must be acknowledged that channel geometry does not remain fixed over time. Rather, it exists in a dynamic equilibrium between competing forces (Stevens et al., 1975; Dethier et al., 2016). If the goal of restoration projects is to restore natural geomorphic processes, the aim of a design should be to restore these processes as expediently as possible (Kondolf et al., 2006; Beechie et al., 2010). Long-term monitoring of a restoration project on the Red River in Idaho found that the accuracy of initial

channel geometries only matters to a point. Channel reaches restored to 96% and 157% of stable widths from effective discharge calculations re-established dynamic equilibrium in the same timeframe. Only a severely over-widened reach designed at 191% of the stable width took longer (Tranmer et al., 2022).

Based on the results of this case study, the accuracy of the stable channel analytical method is suitable for restoration design. It would likely best be used in the conceptual or 30% design phase to gain an understanding of geomorphic processes and to approximate stable channel dimensions. Channel dimensions could then be refined at later design stages using morphodynamic models which directly simulate sediment transport or the CSR method which accounts for flow variability.

CONCLUSION

For decades the stable channel analytical method has been proposed as a simple conceptual framework for determining stable channel geometries. Despite being widely published in design literature from the USACE and USDA, little evidence exists to support its accuracy in gravel-bedded alluvial rivers. This is problematic because error in calculated sediment transport rates, one of the key inputs to this method, can be exceptionally large in these settings. By applying the stable channel analytical method to 22 gravel-bedded rivers across the western United States, it was found to be accurate enough for restoration design. Mean error for depth was on the order of -9% to 32%. Median error for slope was between -3% and 0%. This is better than other comparable methods for sizing gravel-bedded rivers. Method accuracy can be improved by using half-yield discharge instead of design discharge, subsurface gradations instead of surface gradations, and by carefully selecting representative sediment transport equations.

REFERENCES

Abou-Seida, M. M., & Saleh, M. (1987). Design of stable alluvial channels. *Journal of hydraulic research*, *25*(4), 433-446.

Andrews, E. D. (1980). Effective and bankfull discharges of streams in the Yampa River basin, Colorado and Wyoming. *Journal of Hydrology*, *46*(3–4), 311–330. https://doi.org/10.1016/0022-1694(80)90084-0

Andrews, E. D. (1994). Marginal bed load transport in a gravel bed stream, Sagehen Creek, California. *Water Resources Research*, *30*(7), 2241–2250. https://doi.org/10.1029/94WR00553

Beechie, T. J., Liermann, M., Pollock, M. M., Baker, S., & Davies, J. (2006). Channel pattern and river-floodplain dynamics in forested mountain river systems. *Geomorphology*, *78*(1–2), 124–141. https://doi.org/10.1016/j.geomorph.2006.01.030

Beechie, T. J., Sear, D. A., Olden, J. D., Pess, G. R., Buffington, J. M., Moir, H., ... & Pollock, M. M. (2010). Process-based principles for restoring river ecosystems. *BioScience*, *60*(3), 209-222.

Biedenharn, D., Copeland, R., Thorne, C., Soar, P., Hey, R., & Watston, C. (2000). *Effective Discharge Calculation: A Practical Guide* (TR-00-15; p. 48). U.S. Army Engineer Research and Development Center.

Bledsoe, B., Baker, D., Nelson, P., Rosburg, T., Sholtes, J., Stroth, T., National Cooperative Highway Research Program, Transportation Research Board, & National Academies of Sciences, Engineering, and Medicine. (2017). *Guidance for Design Hydrology for Stream Restoration and Channel Stability* (p. 24879). Transportation Research Board. https://doi.org/10.17226/24879

Blench, T. (1951). *Hydraulics of sediment- bearing canals and rivers: Vancouver*. Evans Ind. Ltd

Brown, C. B. (1950). Sediment transportation. In Engineering Hydraulics, ed. H. Rouse. New York: Wiley. pp. 769–857.

Chang, H. H. (1980). Stable Alluvial Canal Design. *Journal of the Hydraulics Division*, *106*(5), 873–891. https://doi.org/10.1061/JYCEAJ.0005429

Chang, H.H. (1998). Fluvial Processes in River Engineering. Krieger Publishing Company, Malabar, FL. 432 pp.

Chien, N. (1956). The present status of research on sediment transport. Trans. ASCE, 121, 833–68.

Copeland, R. (1994). *Application of Channel Stability Methods—Case Studies* (Technical Report HL-94-11; p. 59). U.S. Army Engineers Waterways Experiment Station.

Costa, J.E., O'Connor, J.E., 1995. Geomorphically effective floods. In: Costa, J.E., Miller, A.J., Potter, K.W., Wilcock, P.R. (Eds.), Natural and Anthropogenic Influences in Fluvial Geomorphology, Geophysical Monograph 89. American Geophysical Union, Washington, DC, pp. 45–56.

Davidson, S.L., Eaton, B.C., 2018. Beyond regime: A stochastic model of floods, bank erosion, and channel migration. Water Resour. Res. 54, 6282–6298. https://doi.org/ 10.1029/2017WR022059.

Dethier, E., Magilligan, F.J., Renshaw, C.E., et al., 2016. The role of chronic and episodic disturbances on channel-hillslope coupling: The persistence and legacy of extreme floods. Earth Surf. Process. Landforms 41, 1437–1447

Doyle, M. W., Shields, D., Boyd, K. F., Skidmore, P. B., & Dominick, D. (2007). Channel-Forming Discharge Selection in River Restoration Design. *Journal of Hydraulic Engineering*, *133*(7), 831–837. https://doi.org/10.1061/(ASCE)0733-9429(2007)133:7(831)

Duan, N. (1983). Smearing Estimate: A Nonparametric Retransformation Method. *Journal of the American Statistical Association*, *78*(383), 605–610. https://doi.org/10.1080/01621459.1983.10478017

Dury, G. H. (1973). “Magnitude-frequency analysis and channel morphology.” Fluvial geomorphology: A proceedings volume of the fourth annual geomorphology symposia series. M. Morisawa, ed., Allen and Unwin, Binghampton, New York, 91-121.

Einstein, H. A. (1942). Formulas for the Transportation of Bed Load. *Transactions of the American Society of Civil Engineers*, *107*(1), 561–577. https://doi.org/10.1061/TACEAT.0005468

Einstein, H.A. (1950). The bed-load function for sediment transport in open channel flows. TECHNICAL BULLETIN No. 1026, U.S. Department of Agriculture, Soil Conservation Service

Erwin, S. O., Schmidt, J. C., & Nelson, N. C. (2011). Downstream effects of impounding a natural lake: The Snake River downstream from Jackson Lake Dam, Wyoming, USA: DOWNSTREAM EFFECTS OF IMPOUNDING A NATURAL LAKE. *Earth Surface Processes and Landforms*, *36*(11), 1421–1434. https://doi.org/10.1002/esp.2159

Ferguson, R. I. (2003). The missing dimension: Effects of lateral variation on 1-D calculations of fluvial bedload transport. *Geomorphology*, *56*(1–2), 1–14. https://doi.org/10.1016/S0169-555X(03)00042-4

Gibson, S. (2021). HEC-RAS 1D Sediment Transport – Creating a Sediment Rating Curve (Best Practices). U.S. Army Corps of Engineers. https://www.hec.usace.army.mil/confluence/rasdocs/rassed1d/1d-sediment-transport-user-s-manual/entering-and-editing-sediment-data/sediment-boundary-conditions/rating-curve/creating-a-sediment-rating-curve-best-practices

Gholami, A., Bonakdari, H., Samui, P., Mohammadian, M., & Gharabaghi, B. (2019). Predicting stable alluvial channel profiles using emotional artificial neural networks. *Applied Soft Computing*, *78*, 420–437. https://doi.org/10.1016/j.asoc.2019.03.003

Gholami, A., Bonakdari, H., Zeynoddin, M., Ebtehaj, I., Gharabaghi, B., & Khodashenas, S. R. (2019). Reliable method of determining stable threshold channel shape using experimental and gene expression programming techniques. *Neural Computing and Applications*, *31*(10), 5799–5817. https://doi.org/10.1007/s00521-018-3411-7

Gomez, B., & Church, M. (1989). An assessment of bed load sediment transport formulae for gravel bed rivers. *Water Resources Research*, *25*(6), 1161–1186. https://doi.org/10.1029/WR025i006p01161

Griffiths, G. A. (1981). Stable-channel design in gravel-bed rivers. *Journal of Hydrology*, *52*(3–4), 291–305. https://doi.org/10.1016/0022-1694(81)90176-1

Griffiths, G. A. (1983). Stable-channel design in alluvial rivers. *Journal of Hydrology*, *65*(4), 259–270. https://doi.org/10.1016/0022-1694(83)90080-X

Gray, J.R., & Simoes, F.J.M. (2008). Estimating Sediment Discharge: Appendix D. U.S. Geological Survey and American Society of Civil Engineers. https://pubs.usgs.gov/publication/70120727

Hack, J., & Goodlett, J. (1960). *Geomorphology and Forest Ecology of a Mountain Region in the Central Appalachians* (Professional Paper 347; Professional Paper). U.S. Geological Survey.

Harun, M. A., Ab. Ghani, A., Mohammadpour, R., & Chan, N. W. (2021). GEP- and MLR-based equations for stable channel analysis. *Journal of Hydroinformatics*, *23*(6), 1247–1270. https://doi.org/10.2166/hydro.2021.047

Hey, R. D. (1975). "Design discharge for natural channels," Science, Technology and Environmental Management. R. D. Hey and T. D. Davies, eds., Saxon House, 73-88.

Hey, R. D. (1997). "Channel response and channel forming discharge: literature review and interpretation," Final Report, U.S. Army Contract Number R&D 6871-EN-01.

Inglis, C. (1941). Meandering of Rivers. *Central Board of India*, *Publication 24*, 98–99.

Inglis, C., & Lacey, G. (1947). Meanders and Their Bearing on River Training. *Institution of Civil Engineering, Maritime and Waterways Engineering Division*, *Paper No. 7*.

Julien, P. Y. (2010). *Erosion and Sedimentation* (2nd ed.). Cambridge University Press. https://doi.org/10.1017/CBO9780511806049

King, J. G., Emmett, W. W., Whiting, P., Kenworthy, R., & Barry, J. J. (2004). *Sediment Transport Data and Related Information for Selected Coarse-Bed Streams and Rivers in Idaho* (RMRS-GTR-131; p. 26). U.S. Department of Agriculture, Forest Service, Rocky Mountain Research Station.

Kondolf, G. M., Boulton, A. J., O'Daniel, S., Poole, G. C., Rahel, F. J., Stanley, E. H., ... & Nakamura, K. (2006). Process-based ecological river restoration: visualizing three-dimensional connectivity and dynamic vectors to recover lost linkages. *Ecology and society*, *11*(2).

Leopold, L., & Maddock, T. (1953). *The Hydraulic Geometry of Stream Channels and Some Physiographic Implications*. U.S. Geological Survey.

Leopold, L., & Wolman, G. (1957). *River Channel Patters: Braided, Meandering, and Straight*. U.S. Geological Survey.

López, R., Vericat, D., & Batalla, R. J. (2014). Evaluation of bed load transport formulae in a large regulated gravel bed river: The lower Ebro (NE Iberian Peninsula). *Journal of Hydrology*, *510*, 164–181. https://doi.org/10.1016/j.jhydrol.2013.12.014

Meyer-Peter, E., & Muller, R. (1948). Formulas for Bed-Load Transport. *Proceedings of the 2nd Meeting IAHR*, 39–64.

Monsalve, A., Segura, C., Hucke, N., & Katz, S. (2020). A bed load transport equation based on the spatial distribution of shear stress – Oak Creek revisited. *Earth Surface Dynamics*, *8*(3), 825–839. https://doi.org/10.5194/esurf-8-825-2020

NRCS. (2007). Chapter 9—Alluvial Channel Design. In *National Engineering Handbook Part 654* (p. 54).

Parker, G., Klingeman, P.C., and McLean, D.G. (1982). *Bedload and size distribution in paved gravel-bed streams*. JOURNAL OF THE HYDRAULICS DIVISION, ASCE. Vol. 108. No. HY4. pp. 544-571.

Ryan, S. E., Porth, L. S., & Troendle, C. A. (2002). Defining phases of bedload transport using piecewise regression. *Earth Surface Processes and Landforms*, *27*(9), 971–990. https://doi.org/10.1002/esp.387

Ryan, S. E., Porth, L. S., & Troendle, C. A. (2005). Coarse sediment transport in mountain streams in Colorado and Wyoming, USA. *Earth Surface Processes and Landforms*, *30*(3), 269–288. https://doi.org/10.1002/esp.1128

Schumm, S. A., Harvey, M. D., & Watson, C. C. (1984). Incised channels: morphology, dynamics, and control.

Sholtes, J., Werbylo, K., & Bledsoe, B. (2014). Physical context for theoretical approaches to sediment transport magnitude-frequency analysis in alluvial channels. *Water Resources Research*, *50*(10), 7900–7914. https://doi.org/10.1002/2014WR015639

Sholtes, J., & Bledsoe, B. (2016). Half-Yield Discharge: Process-Based Predictor of Bankfull Discharge. *Journal of Hydraulic Engineering*, *142*(8).

Stevens, M.A., Simons, D.B., Richardson, E.V., 1975. Nonequilibrium river form. J. Hydraul. Div. Am. Soc. Civ. Eng. 101, 557–566.

Soar, P., & Thorne, C. (2001). *Channel Restoration Design for Meandering Rivers* (ERDC/CHL CR-01-1; p. 454). U.S. Army Engineer Research and Development Center.

Tranmer, A. W., Caamaño, D., Clayton, S. R., Giglou, A. N., Goodwin, P., Buffington, J. M., & Tonina, D. (2022). Testing the effective-discharge paradigm in gravel-bed river restoration. *Geomorphology*, *403*, 108139.

Vanoni, V. (1960). *Sediment Transport and Channel Stability*.

White, W. R., Bettess, R., & Paris, E. (1982). Analytical Approach to River Regime. *Journal of the Hydraulics Division*, *108*(10), 1179–1193. https://doi.org/10.1061/JYCEAJ.0005914

Whiting, P. J., Stamm, J. F., Moog, D. B., & Orndorff, R. L. (1999). Sediment-transporting flows in headwater streams. *Geological Society of America Bulletin*, *111*(3), 450-466.

Wilcock, P. R., & Crowe, J. C. (2003). Surface-based Transport Model for Mixed-Size Sediment. *Journal of Hydraulic Engineering*, *129*(2), 120–128. https://doi.org/10.1061/(ASCE)0733-9429(2003)129:2(120)

Williams, G. P. (1978). Bank-full discharge of rivers. *Water Resources Research*, *14*(6), 1141–1154. https://doi.org/10.1029/WR014i006p01141

Wohl, E., Kramer, N., Ruiz-Villanueva, V., Scott, D. N., Comiti, F., Gurnell, A. M., Piegay, H., Lininger, K. B., Jaeger, K. L., Walters, D. M., & Fausch, K. D. (2019). The Natural Wood Regime in Rivers. *BioScience*, *69*(4), 259–273. https://doi.org/10.1093/biosci/biz013

Wolman, G., & Miller, J. (1960). Magnitude and Frequency of Forces in Geomorphic Processes. *Journal of Geology*, *68*, 54–74.

Yevjevich, V. (1972). *Probability and Statistics in Hydrology*. Water Resources Publications.

Appendix A

Individual Site Analyses

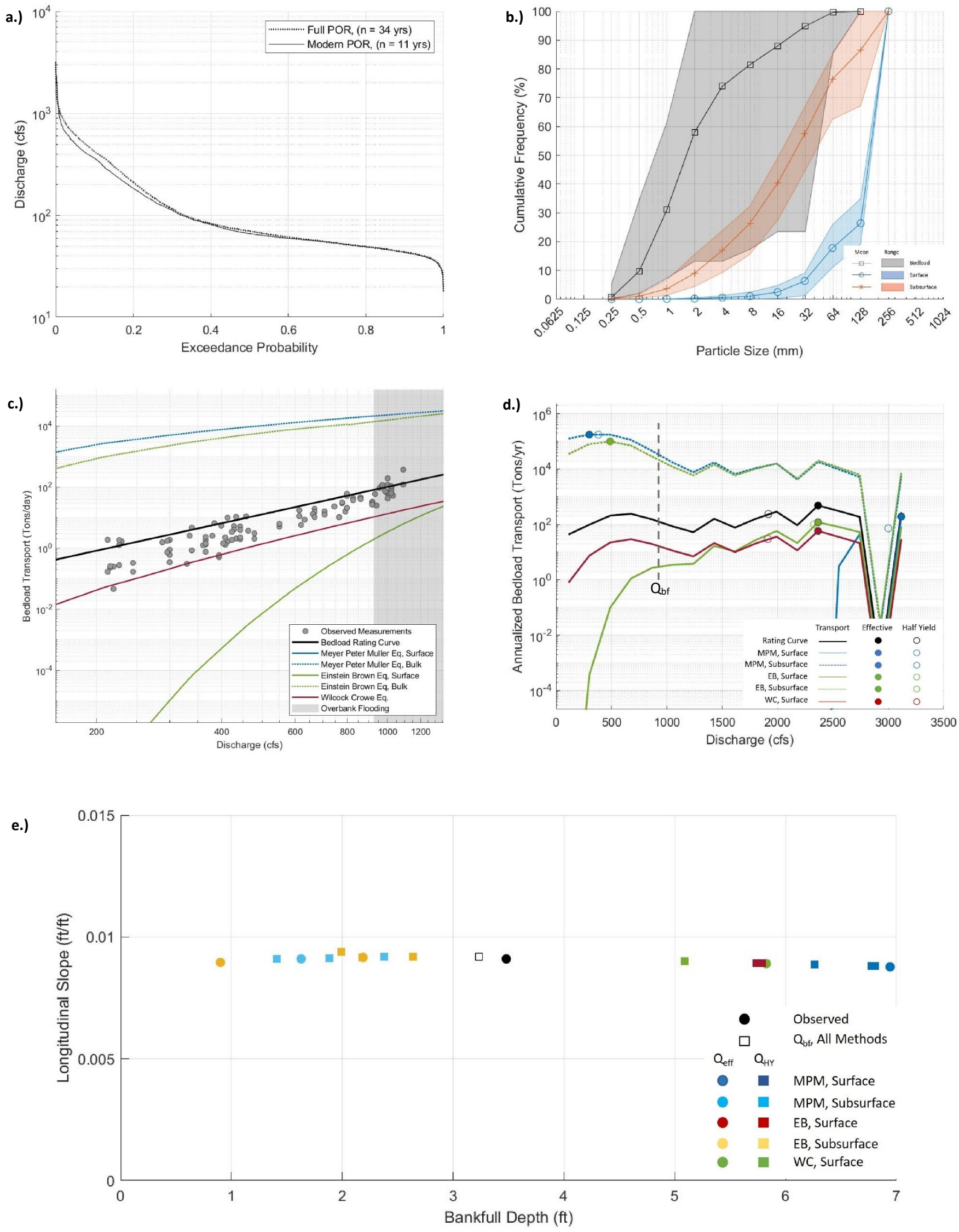

Figure A.1: *Results of analytical channel design procedure for Big Wood Creek, ID showing a.) flow duration curve for full gage history and modern period of record used in analysis, b.) observed sediment and bedload gradations, c.) observed and calculated sediment rating curves, d.) calculated effective and half-yield discharges, and e.) calculated stable geometries compared to observed bankfull geometry.*

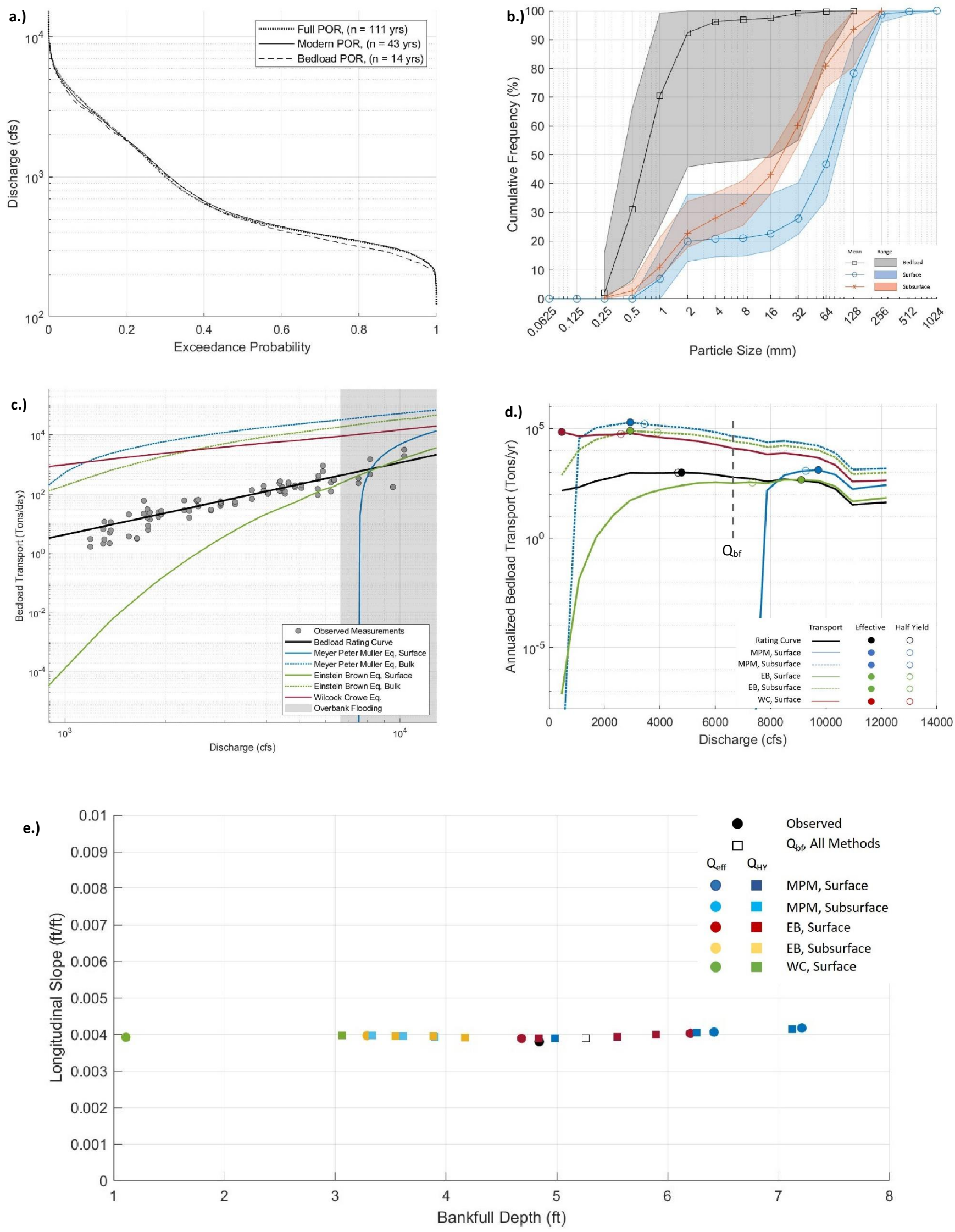

Figure A.2: *Results of analytical channel design procedure for Boise River, ID showing a.) flow duration curve for full gage history and modern period of record used in analysis, b.) observed sediment and bedload gradations, c.) observed and calculated sediment rating curves, d.) calculated effective and half-yield discharges, and e.) calculated stable geometries compared to observed bankfull geometry.*

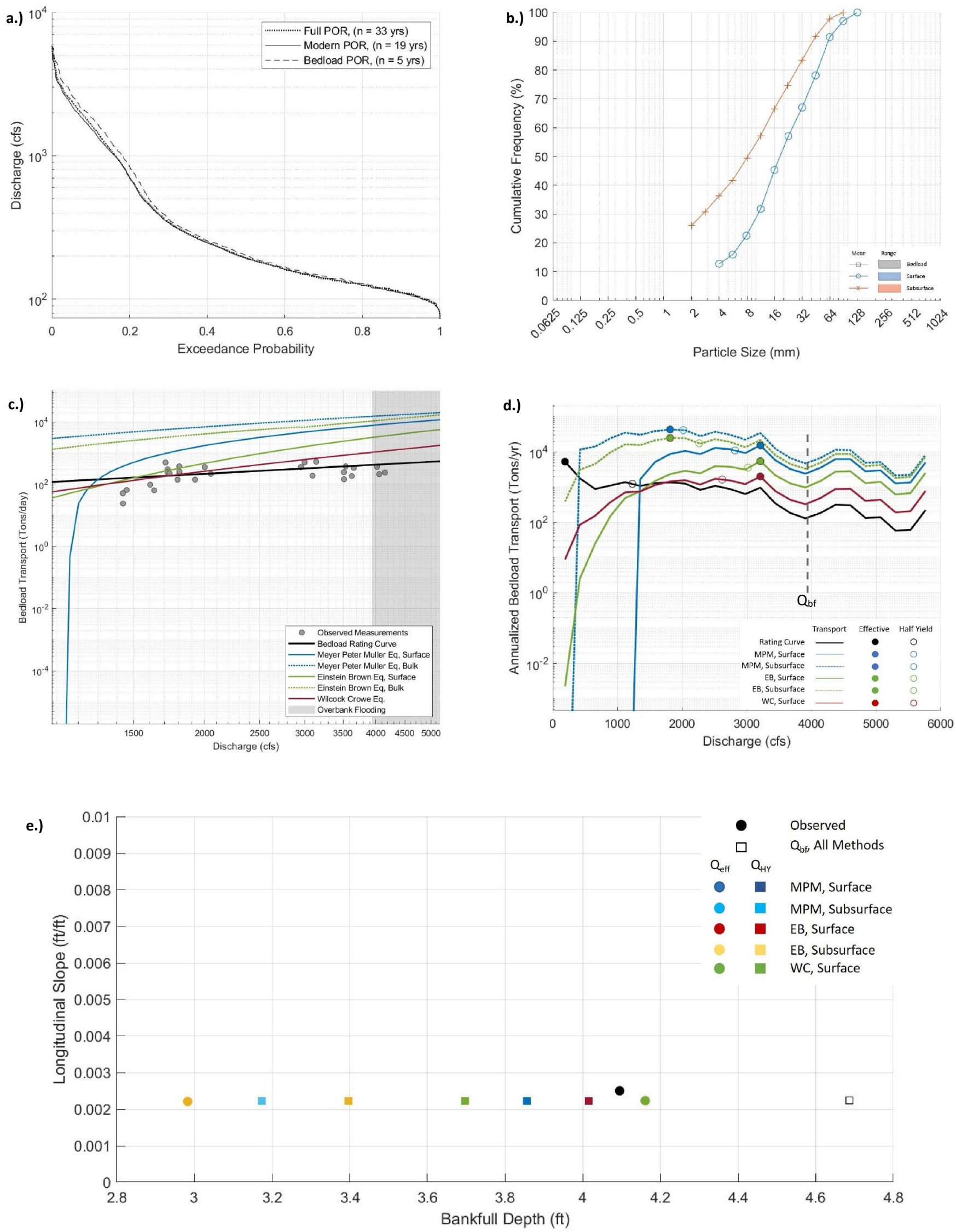

Figure A.3: *Results of analytical channel design procedure for Buffalo Fork, WY showing a.) flow duration curve for full gage history and modern period of record used in analysis, b.) observed sediment and bedload gradations, c.) observed and calculated sediment rating curves, d.) calculated effective and half-yield discharges, and e.) calculated stable geometries compared to observed bankfull geometry.*

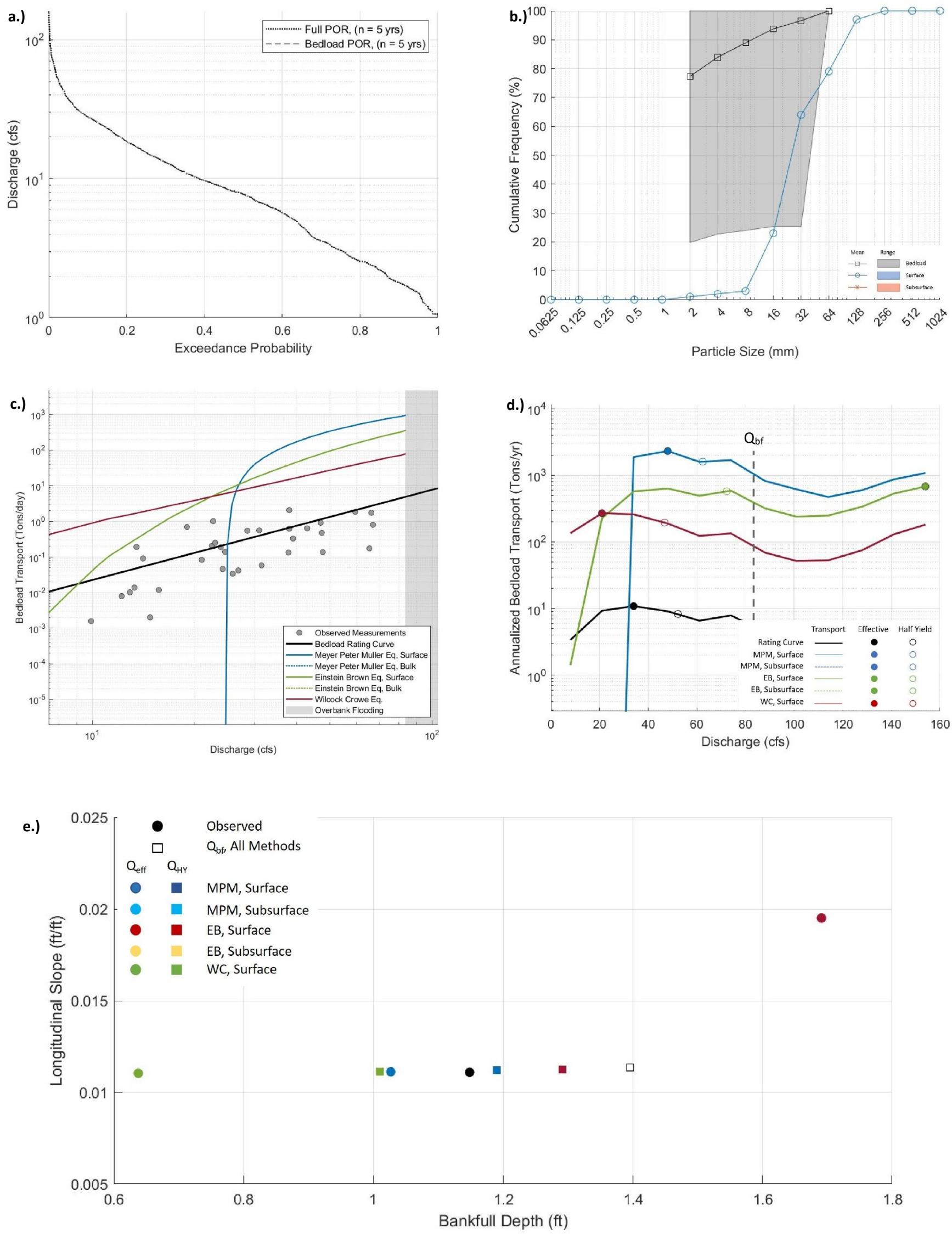

Figure A.4: *Results of analytical channel design procedure for Cat Spur Creek, ID showing a.) flow duration curve for full gage history and modern period of record used in analysis, b.) observed sediment and bedload gradations, c.) observed and calculated sediment rating curves, d.) calculated effective and half-yield discharges, and e.) calculated stable geometries compared to observed bankfull geometry.*

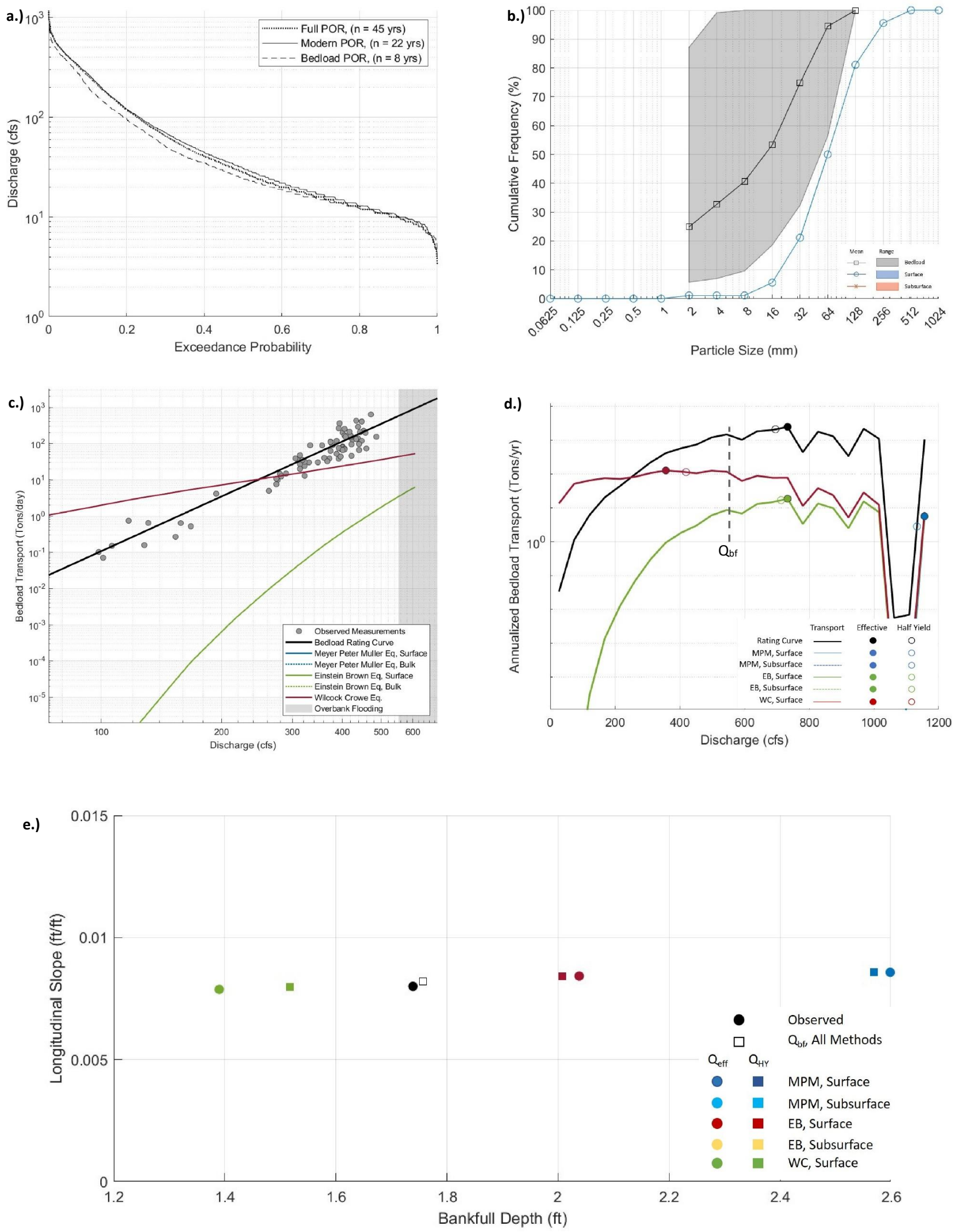

Figure A.5: *Results of analytical channel design procedure for East Fork San Juan River, CO showing a.) flow duration curve for full gage history and modern period of record used in analysis, b.) observed sediment and bedload gradations, c.) observed and calculated sediment rating curves, d.) calculated effective and half-yield discharges, and e.) calculated stable geometries compared to observed bankfull geometry.*

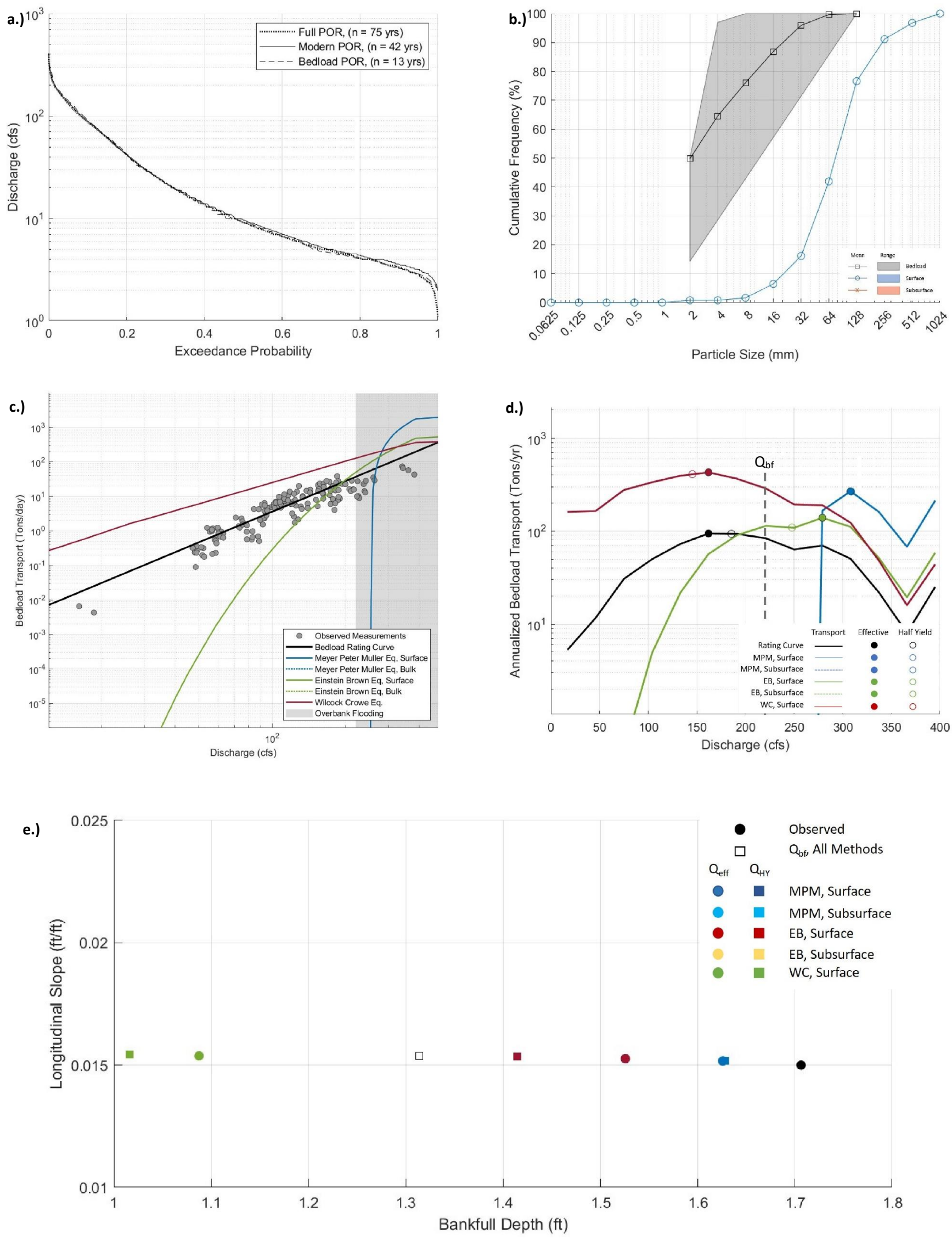

Figure A.6: *Results of analytical channel design procedure for Halfmoon Creek, CO showing a.) flow duration curve for full gage history and modern period of record used in analysis, b.) observed sediment and bedload gradations, c.) observed and calculated sediment rating curves, d.) calculated effective and half-yield discharges, and e.) calculated stable geometries compared to observed bankfull geometry.*

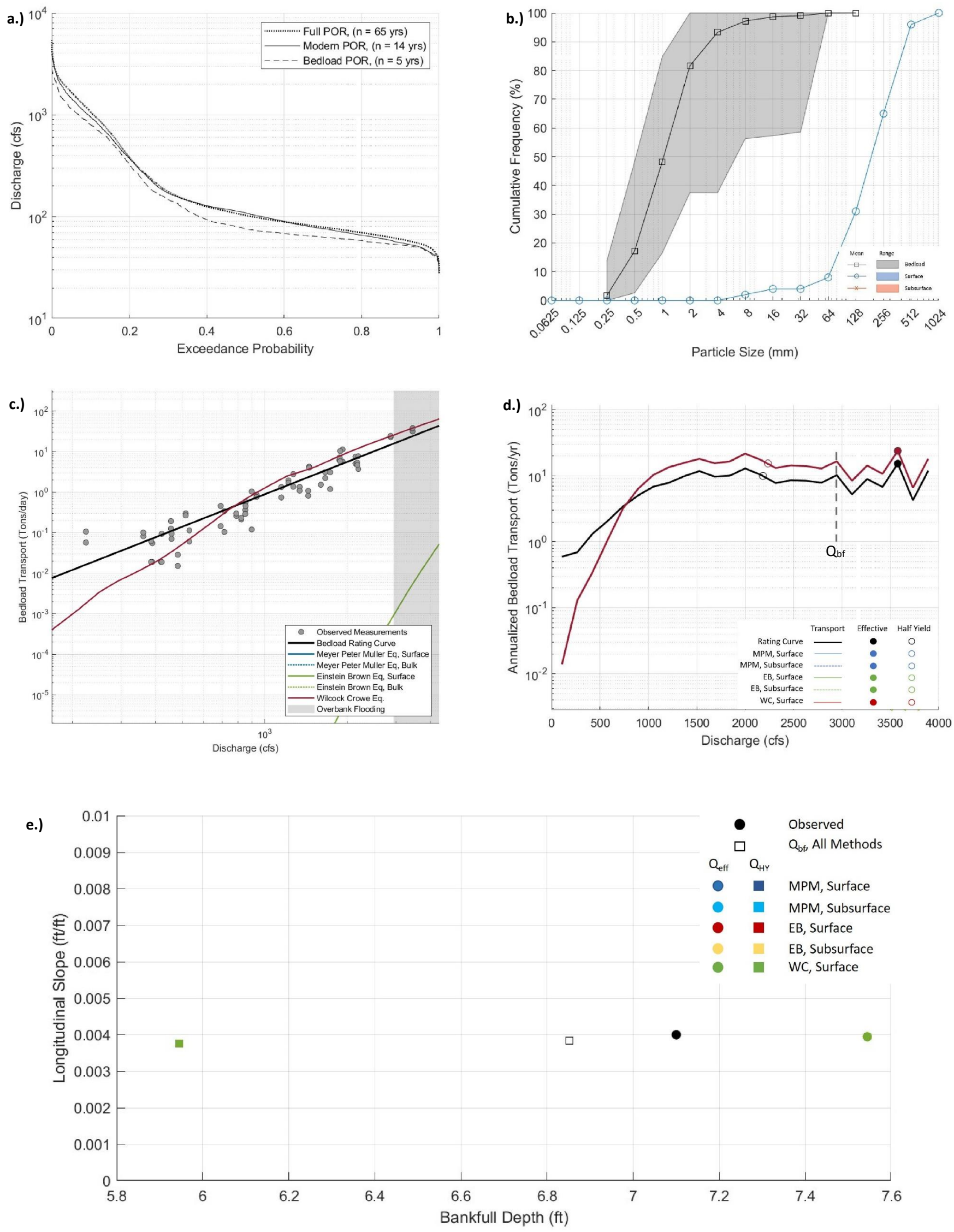

Figure A.7: *Results of analytical channel design procedure for Johnson Creek, ID showing a.) flow duration curve for full gage history and modern period of record used in analysis, b.) observed sediment and bedload gradations, c.) observed and calculated sediment rating curves, d.) calculated effective and half-yield discharges, and e.) calculated stable geometries compared to observed bankfull geometry.*

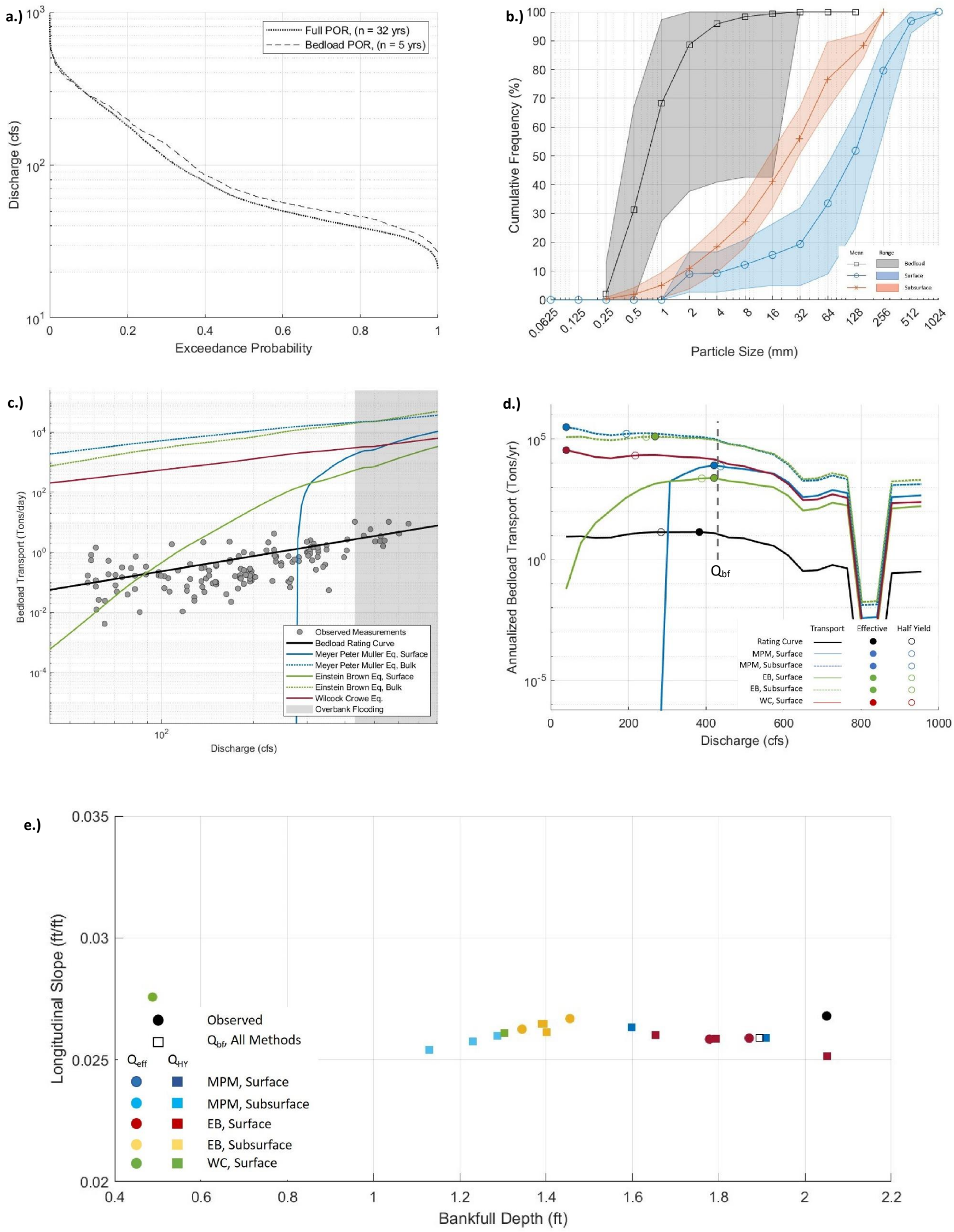

Figure A.8: *Results of analytical channel design procedure for Little Slate Creek, ID showing a.) flow duration curve for full gage history and modern period of record used in analysis, b.) observed sediment and bedload gradations, c.) observed and calculated sediment rating curves, d.) calculated effective and half-yield discharges, and e.) calculated stable geometries compared to observed bankfull geometry.*

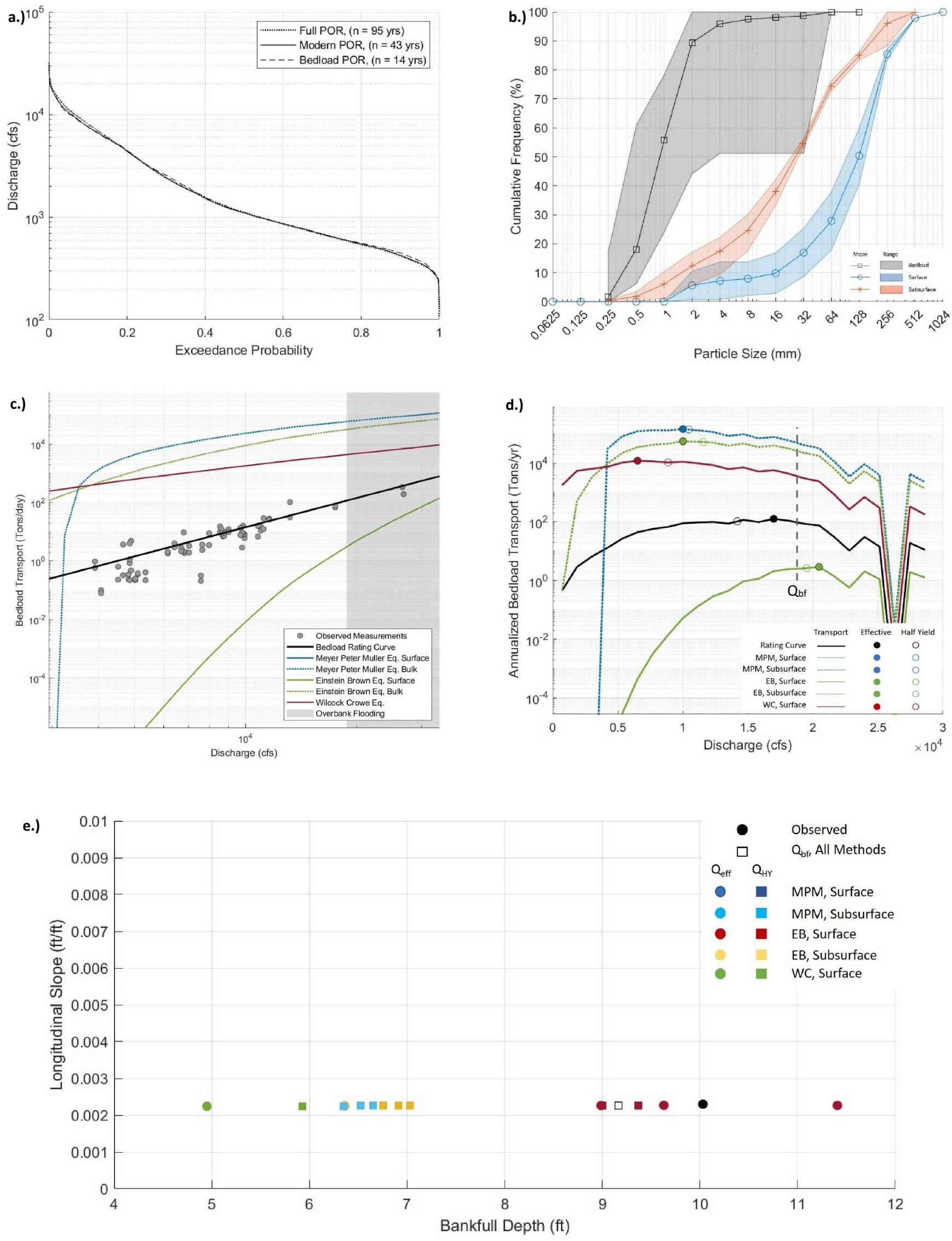

Figure A.9: *Results of analytical channel design procedure for Lochsa River, ID showing a.) flow duration curve for full gage history and modern period of record used in analysis, b.) observed sediment and bedload gradations, c.) observed and calculated sediment rating curves, d.) calculated effective and half-yield discharges, and e.) calculated stable geometries compared to observed bankfull geometry.*

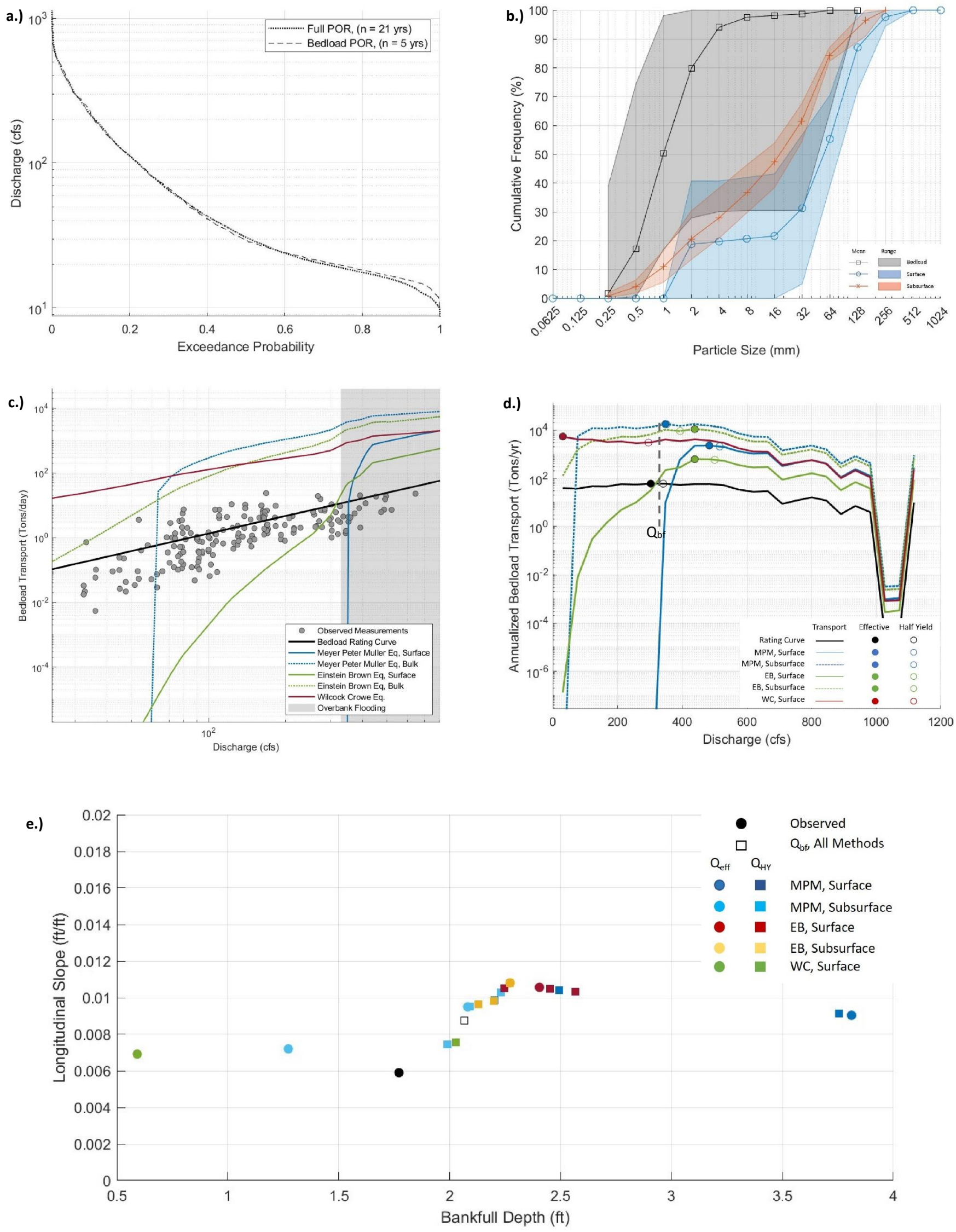

Figure A.10: *Results of analytical channel design procedure for Middle Fork Red River, ID showing a.) flow duration curve for full gage history and modern period of record used in analysis, b.) observed sediment and bedload gradations, c.) observed and calculated sediment rating curves, d.) calculated effective and half-yield discharges, and e.) calculated stable geometries compared to observed bankfull geometry.*

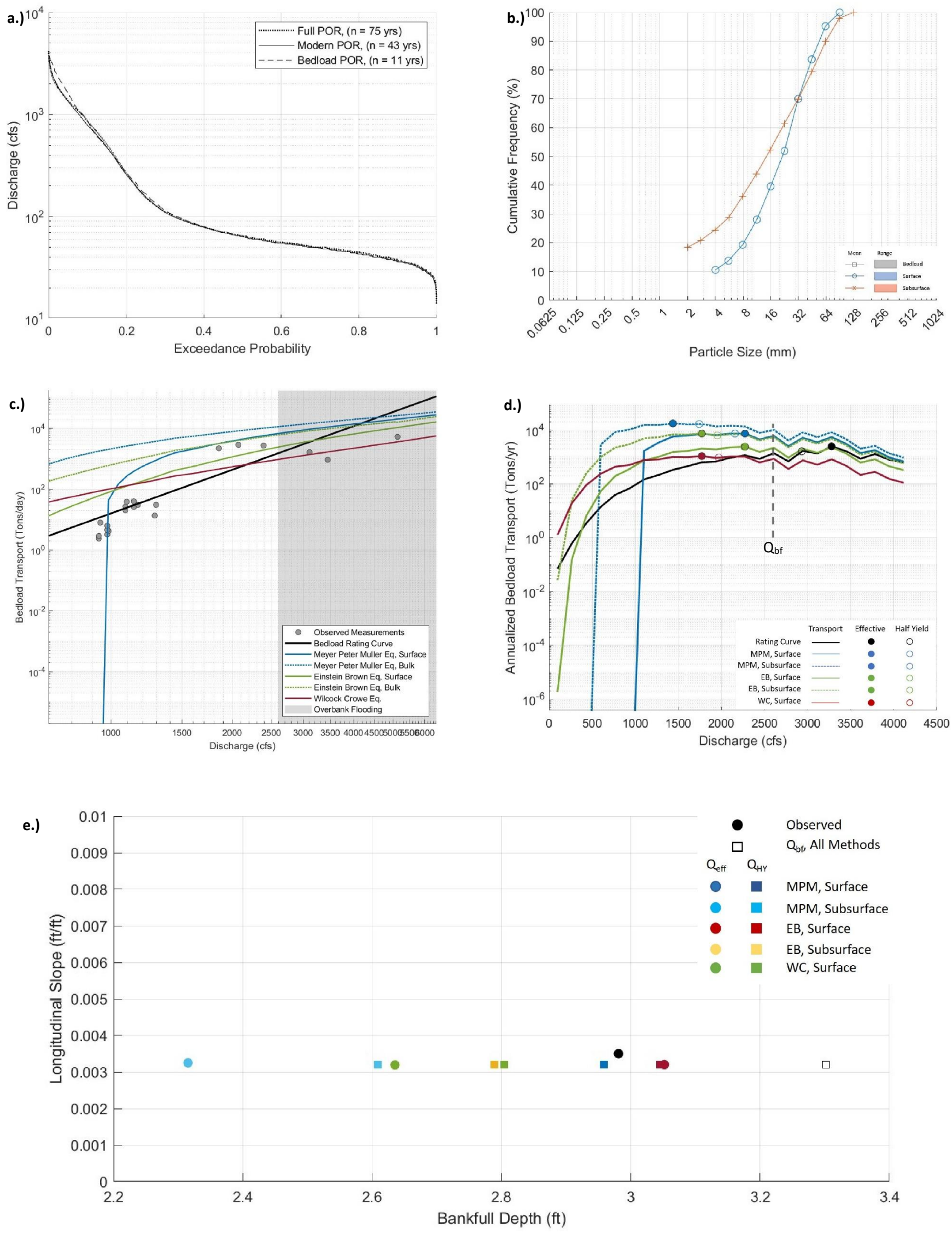

Figure A.11: *Results of analytical channel design procedure for Pacific Creek, WY showing a.) flow duration curve for full gage history and modern period of record used in analysis, b.) observed sediment and bedload gradations, c.) observed and calculated sediment rating curves, d.) calculated effective and half-yield discharges, and e.) calculated stable geometries compared to observed bankfull geometry.*

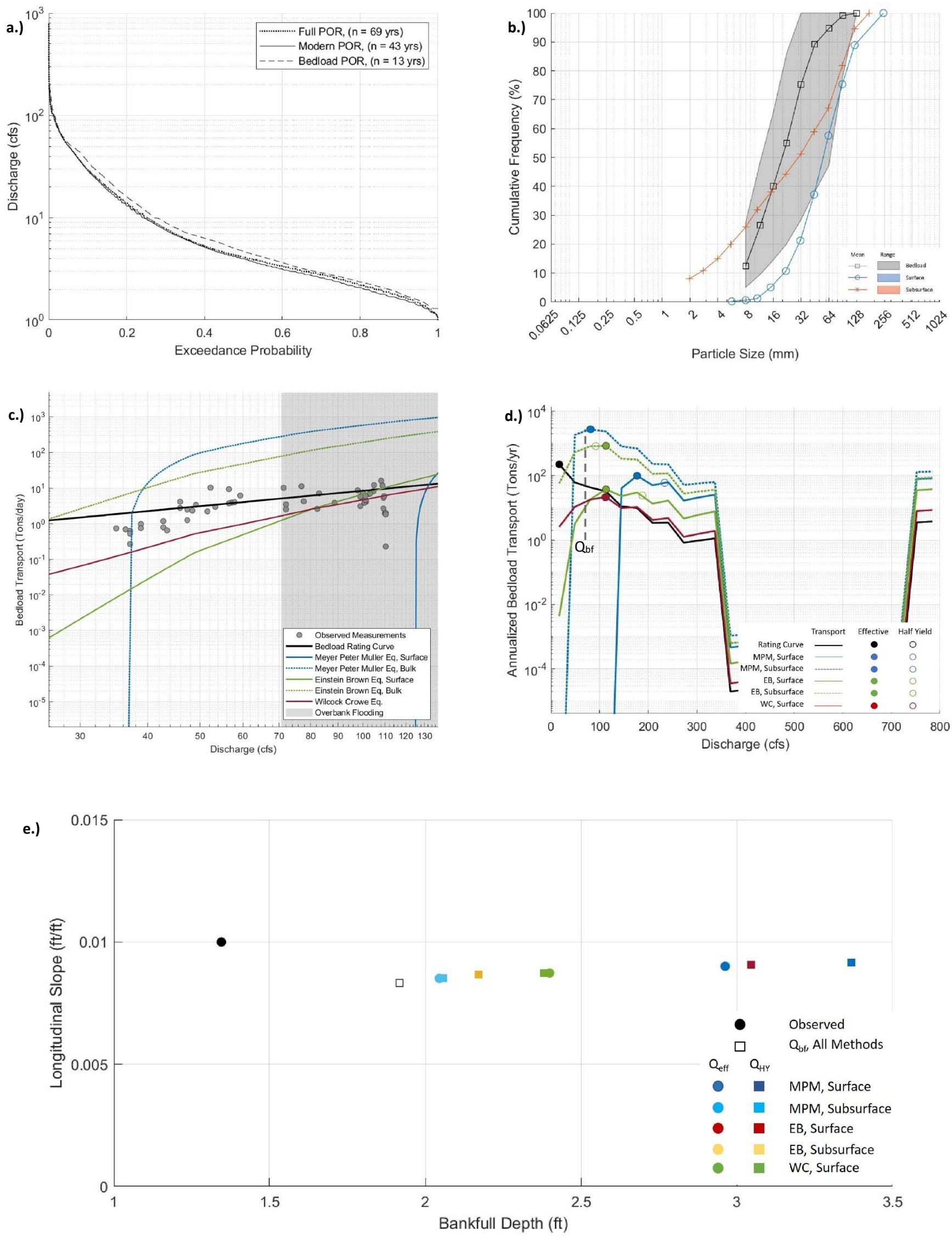

Figure A.12: *Results of analytical channel design procedure for Sagehen Creek, CA showing a.) flow duration curve for full gage history and modern period of record used in analysis, b.) observed sediment and bedload gradations, c.) observed and calculated sediment rating curves, d.) calculated effective and half-yield discharges, and e.) calculated stable geometries compared to observed bankfull geometry.*

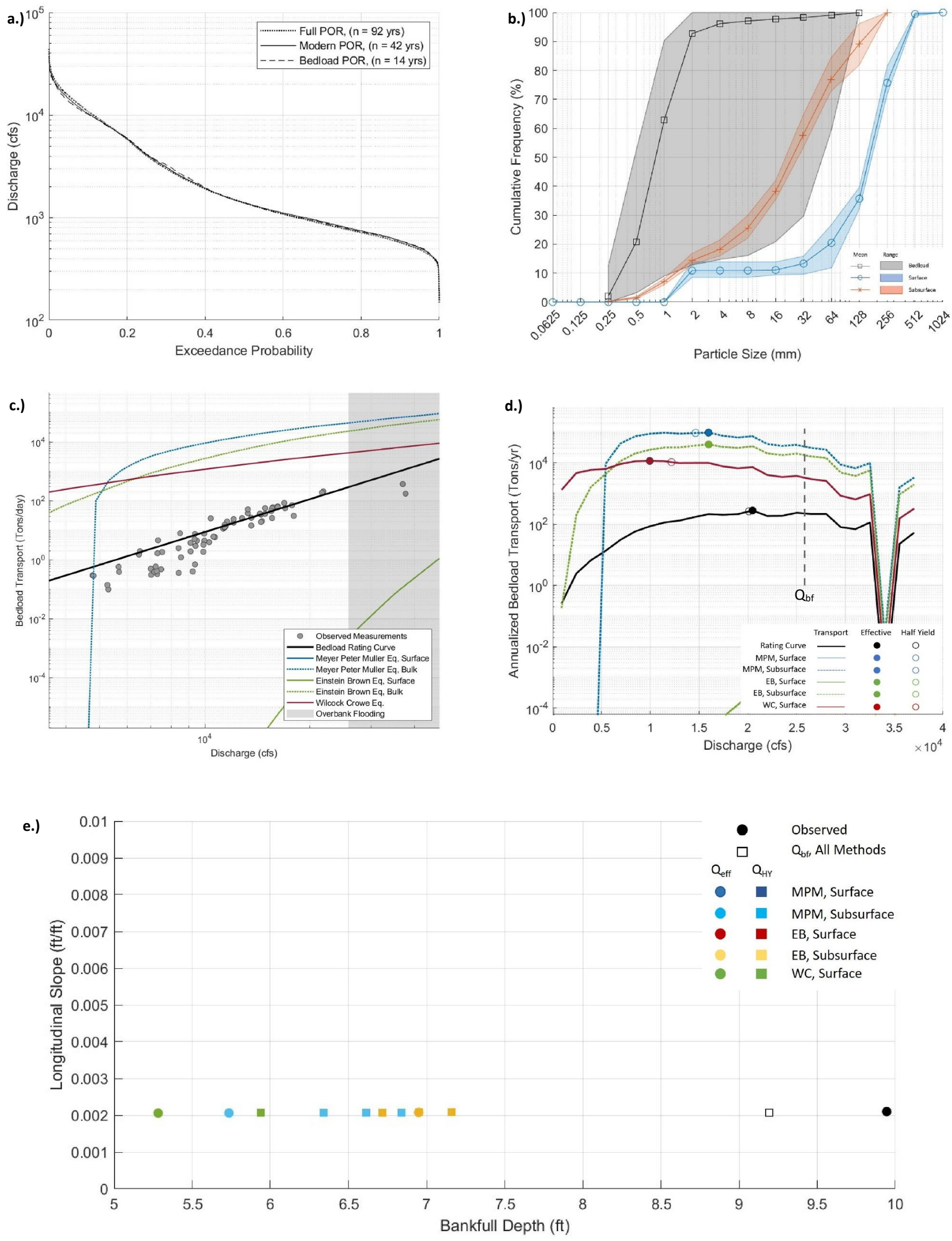

Figure A.13: *Results of analytical channel design procedure for Selway River, ID showing a.) flow duration curve for full gage history and modern period of record used in analysis, b.) observed sediment and bedload gradations, c.) observed and calculated sediment rating curves, d.) calculated effective and half-yield discharges, and e.) calculated stable geometries compared to observed bankfull geometry.*

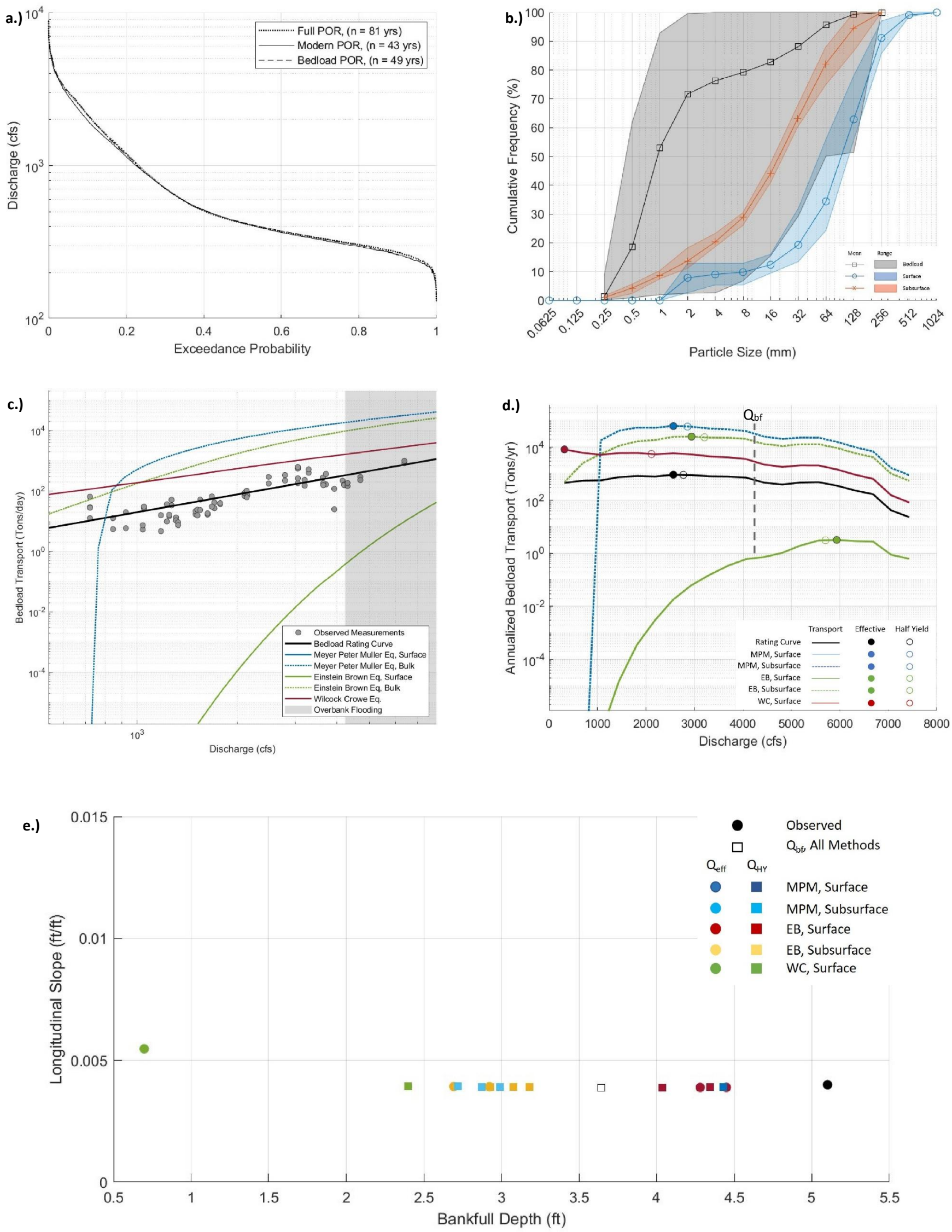

Figure A.14: *Results of analytical channel design procedure for South Fork Payette River, ID showing a.) flow duration curve for full gage history and modern period of record used in analysis, b.) observed sediment and bedload gradations, c.) observed and calculated sediment rating curves, d.) calculated effective and half-yield discharges, and e.) calculated stable geometries compared to observed bankfull geometry.*

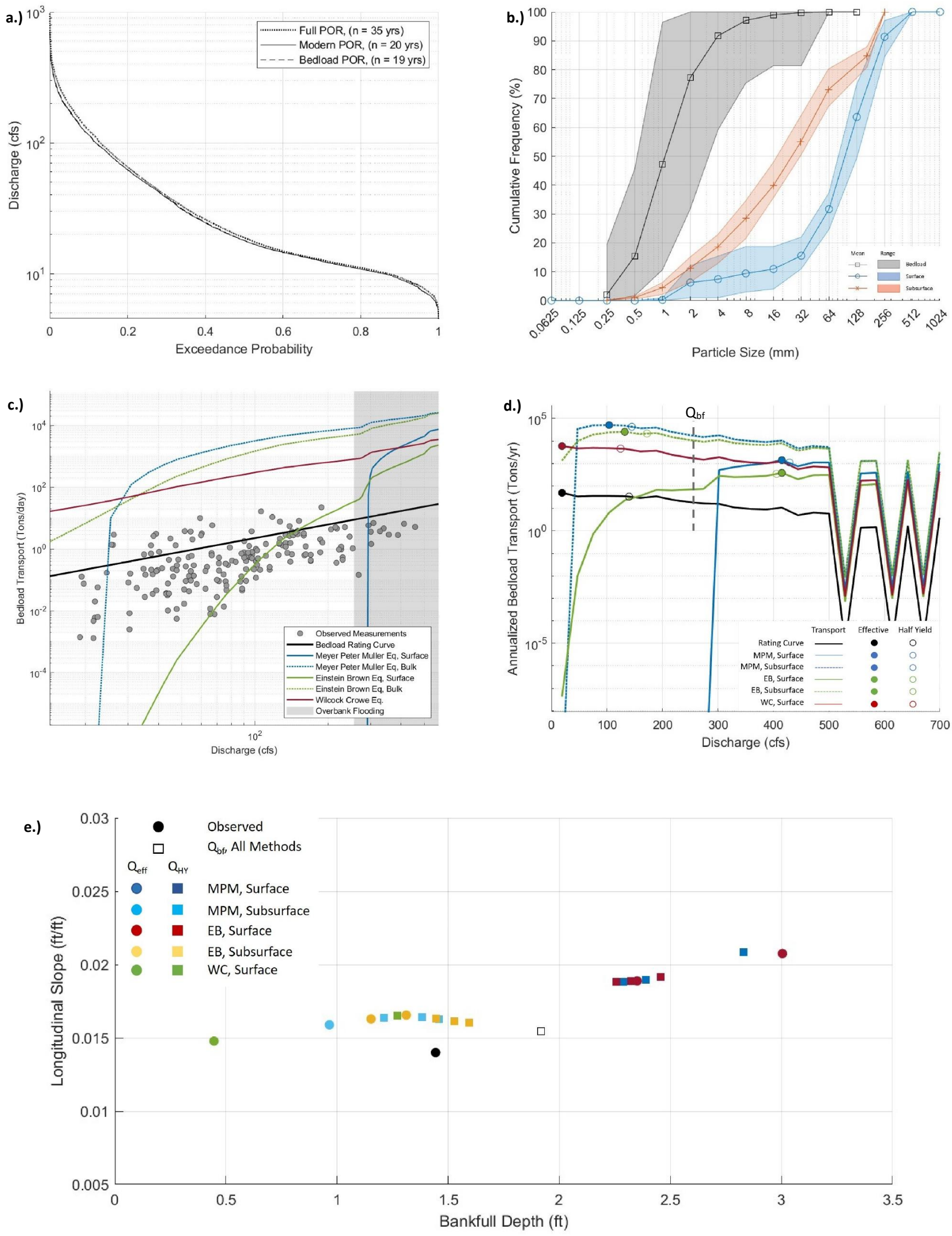

Figure A.15: *Results of analytical channel design procedure for South Fork Red River, ID showing a.) flow duration curve for full gage history and modern period of record used in analysis, b.) observed sediment and bedload gradations, c.) observed and calculated sediment rating curves, d.) calculated effective and half-yield discharges, and e.) calculated stable geometries compared to observed bankfull geometry.*

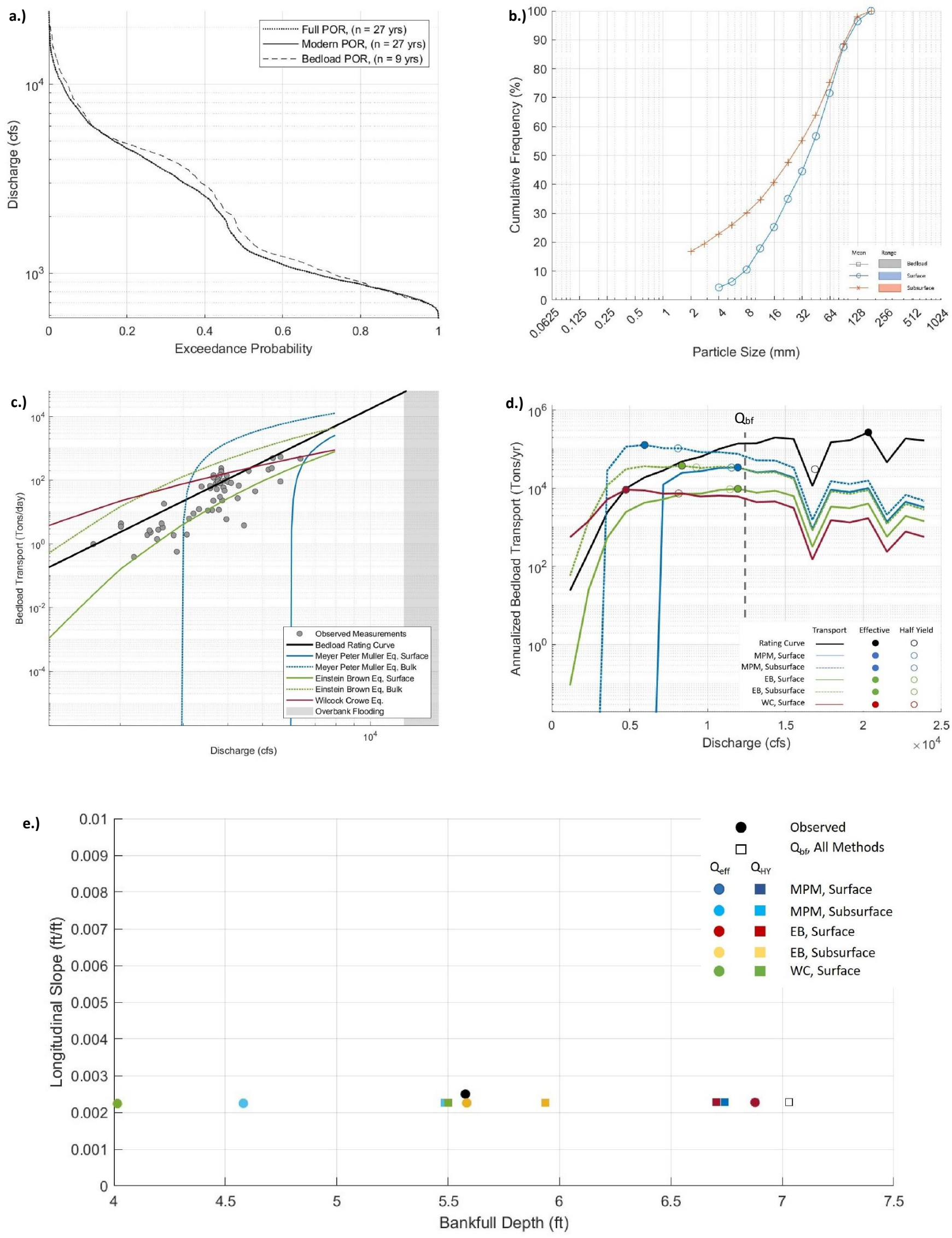

Figure A.16: *Results of analytical channel design procedure for Snake River, WY showing a.) flow duration curve for full gage history and modern period of record used in analysis, b.) observed sediment and bedload gradations, c.) observed and calculated sediment rating curves, d.) calculated effective and half-yield discharges, and e.) calculated stable geometries compared to observed bankfull geometry.*

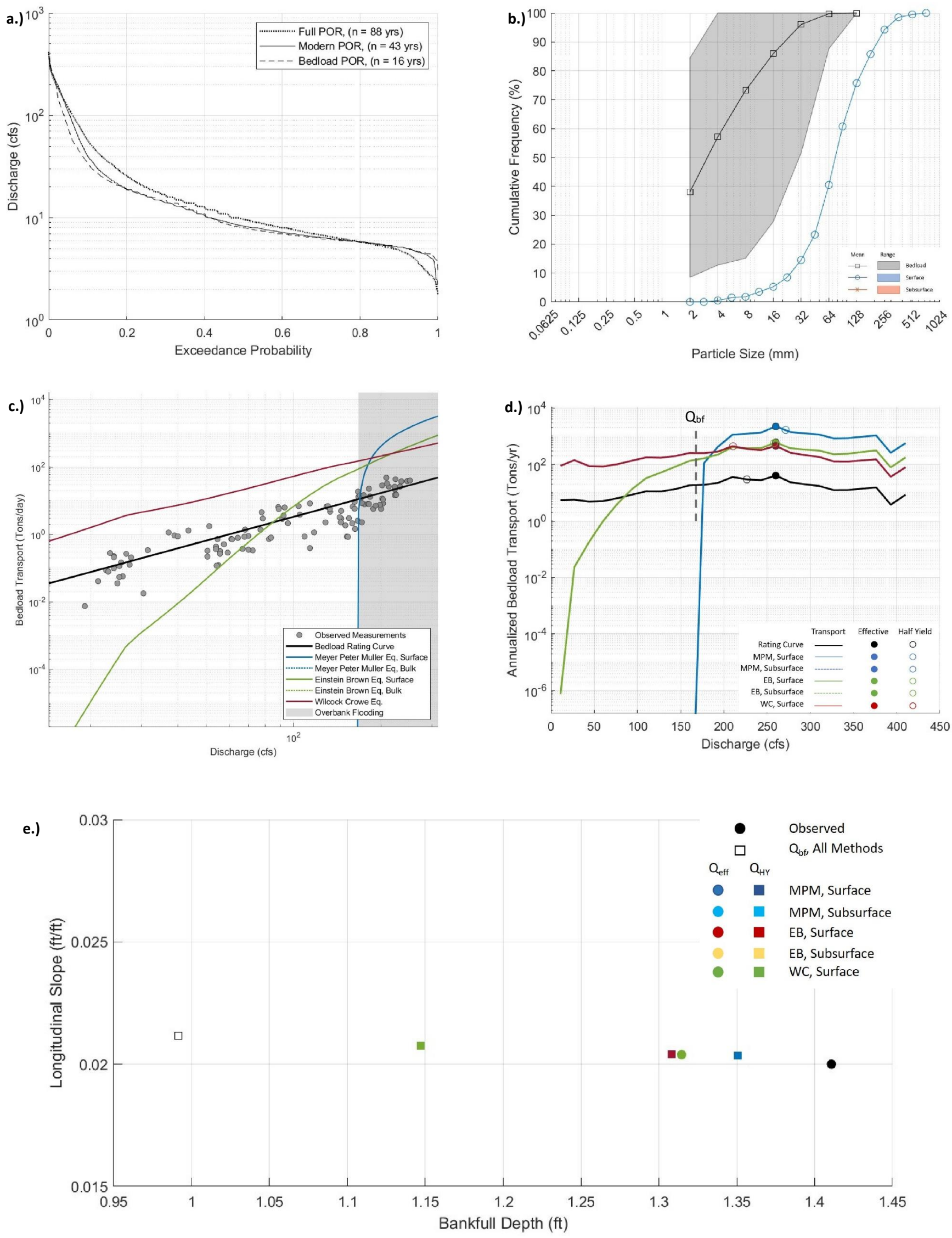

Figure A.17: *Results of analytical channel design procedure for St. Louis Creek Site No. 2, CO showing a.) flow duration curve for full gage history and modern period of record used in analysis, b.) observed sediment and bedload gradations, c.) observed and calculated sediment rating curves, d.) calculated effective and half-yield discharges, and e.) calculated stable geometries compared to observed bankfull geometry.*

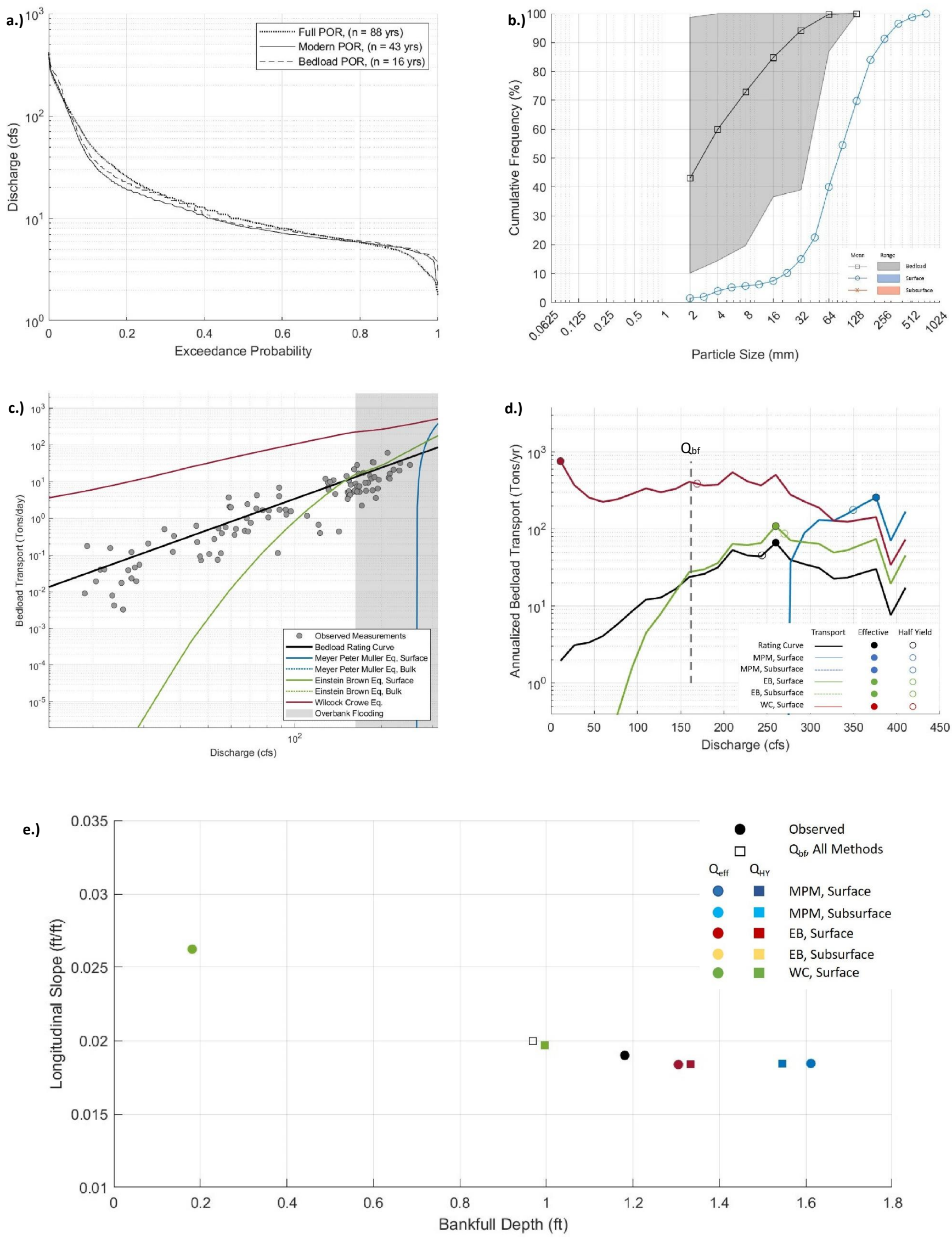

Figure A.18: *Results of analytical channel design procedure for St. Louis Creek Site No 3, CO showing a.) flow duration curve for full gage history and modern period of record used in analysis, b.) observed sediment and bedload gradations, c.) observed and calculated sediment rating curves, d.) calculated effective and half-yield discharges, and e.) calculated stable geometries compared to observed bankfull geometry.*

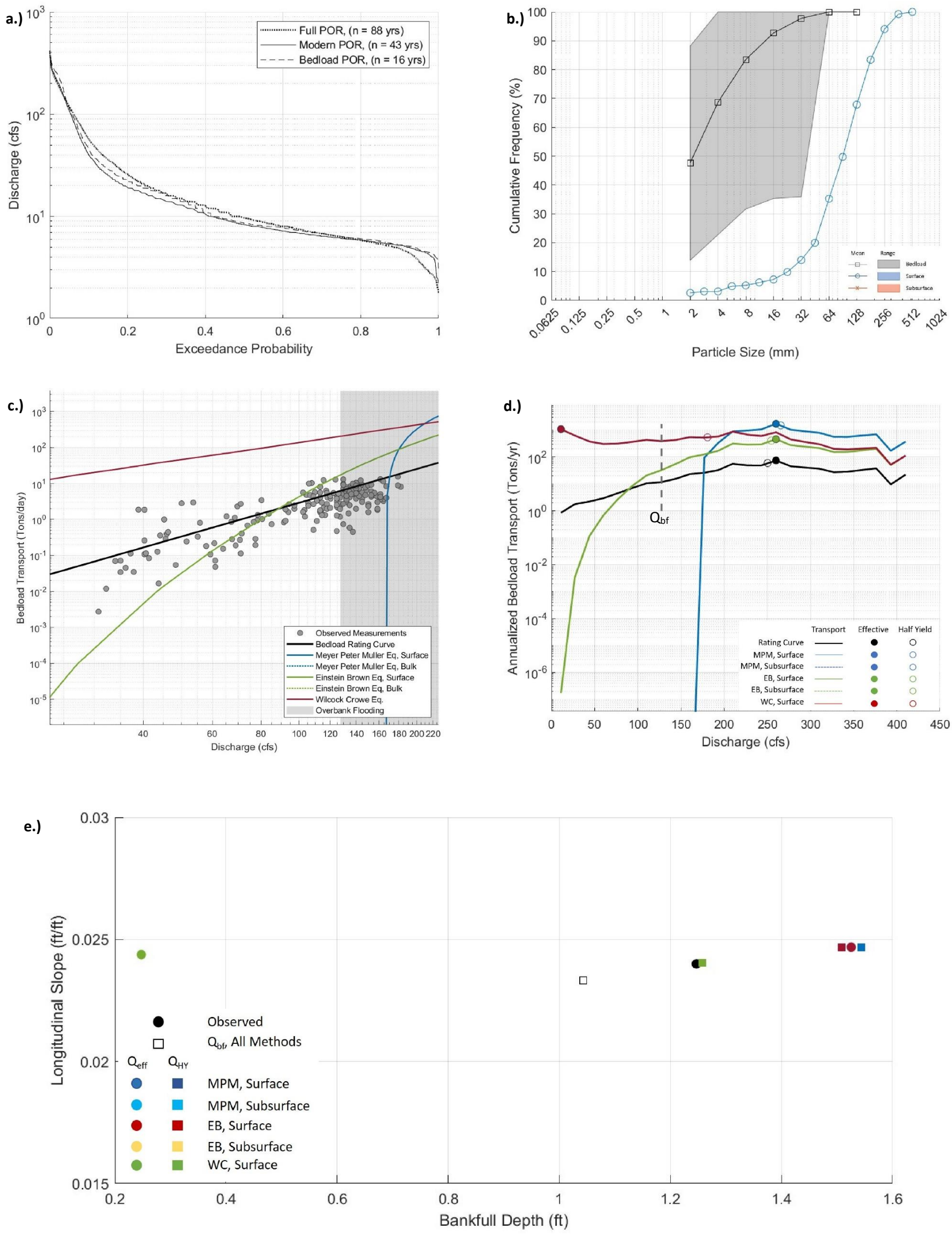

Figure A.19: *Results of analytical channel design procedure for St. Louis Creek Site No. 4a, CO showing a.) flow duration curve for full gage history and modern period of record used in analysis, b.) observed sediment and bedload gradations, c.) observed and calculated sediment rating curves, d.) calculated effective and half-yield discharges, and e.) calculated stable geometries compared to observed bankfull geometry.*

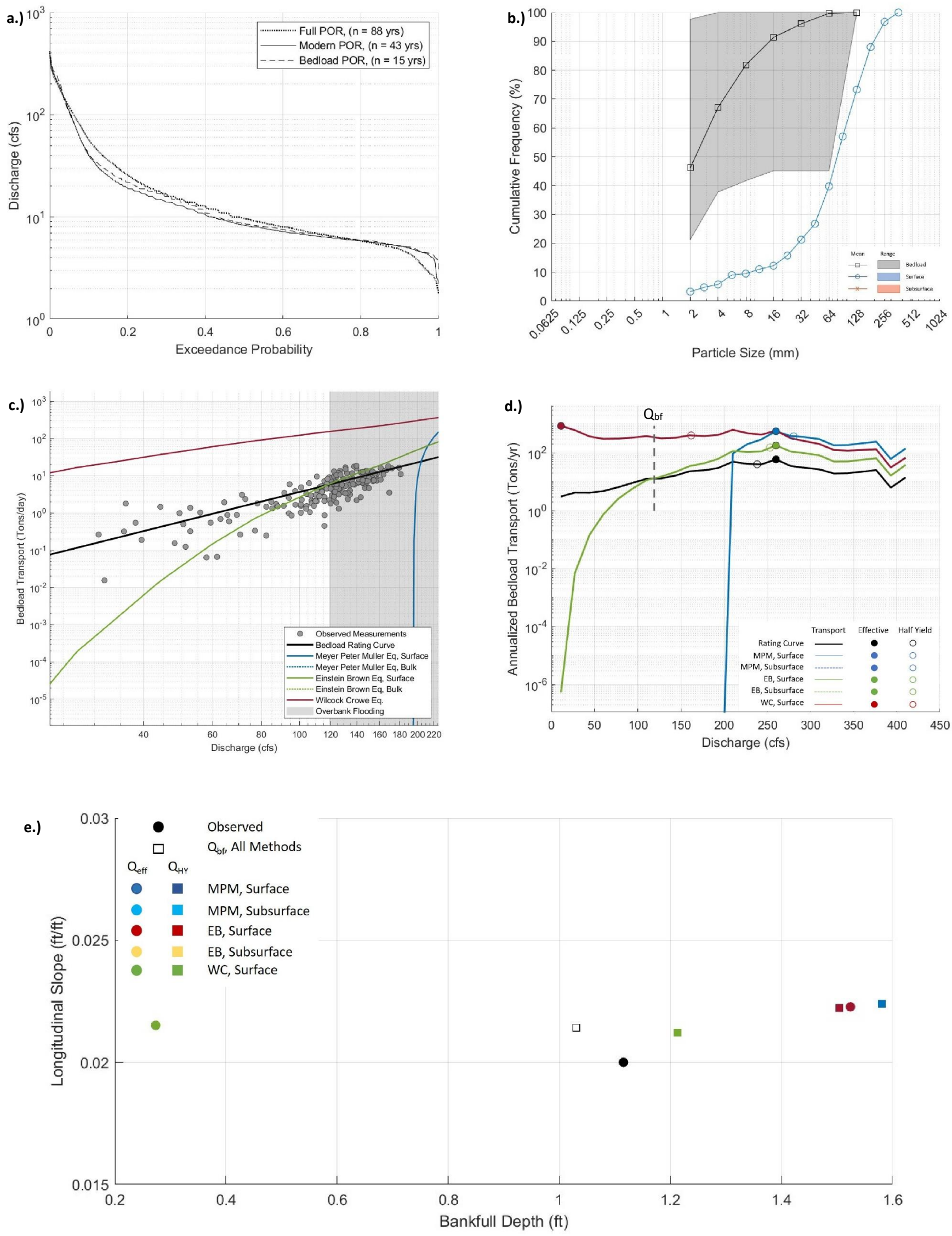

Figure A.20: *Results of analytical channel design procedure for St. Louis Creek Site No. 4b, CO showing a.) flow duration curve for full gage history and modern period of record used in analysis, b.) observed sediment and bedload gradations, c.) observed and calculated sediment rating curves, d.) calculated effective and half-yield discharges, and e.) calculated stable geometries compared to observed bankfull geometry.*

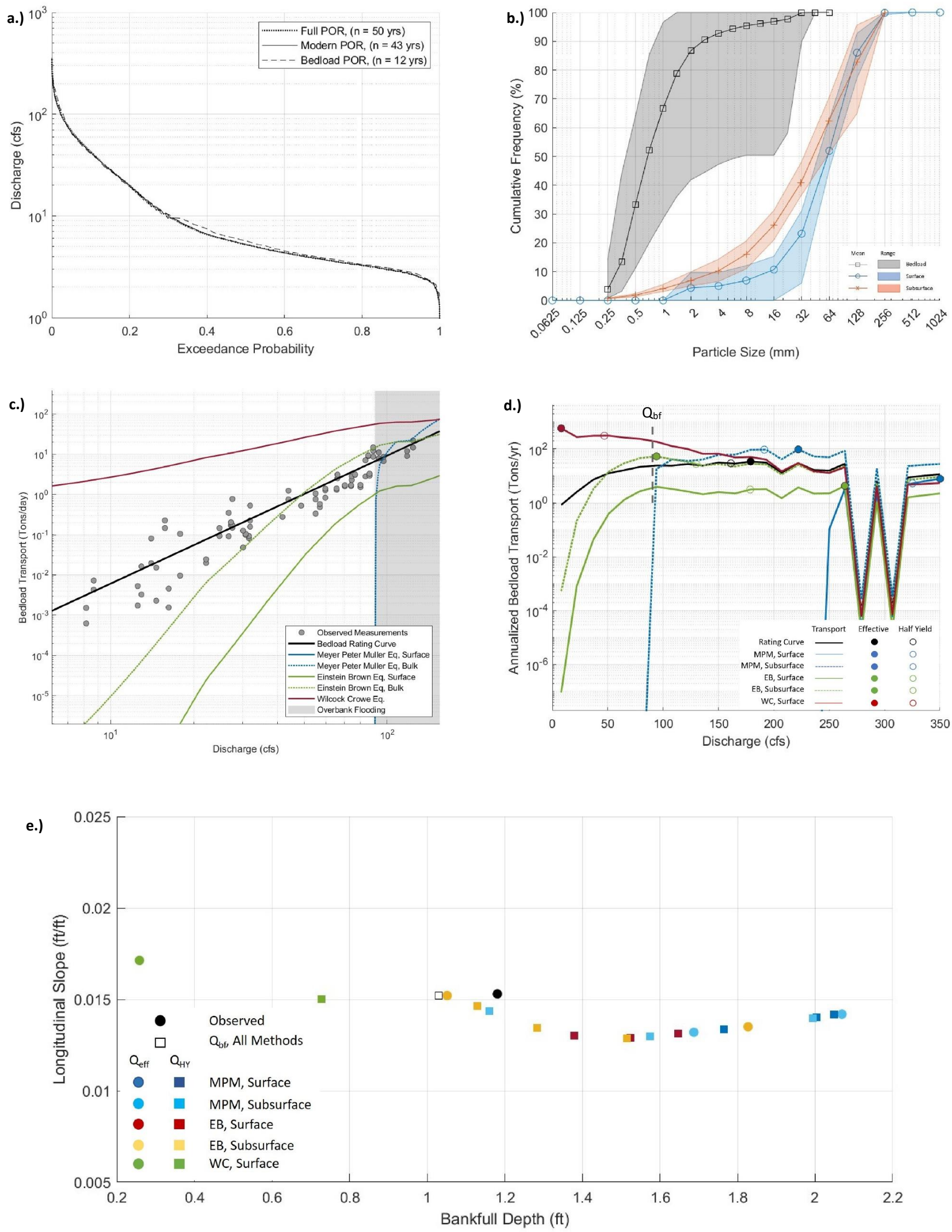

Figure A.21: *Results of analytical channel design procedure for Thompson Creek, ID showing a.) flow duration curve for full gage history and modern period of record used in analysis, b.) observed sediment and bedload gradations, c.) observed and calculated sediment rating curves, d.) calculated effective and half-yield discharges, and e.) calculated stable geometries compared to observed bankfull geometry.*

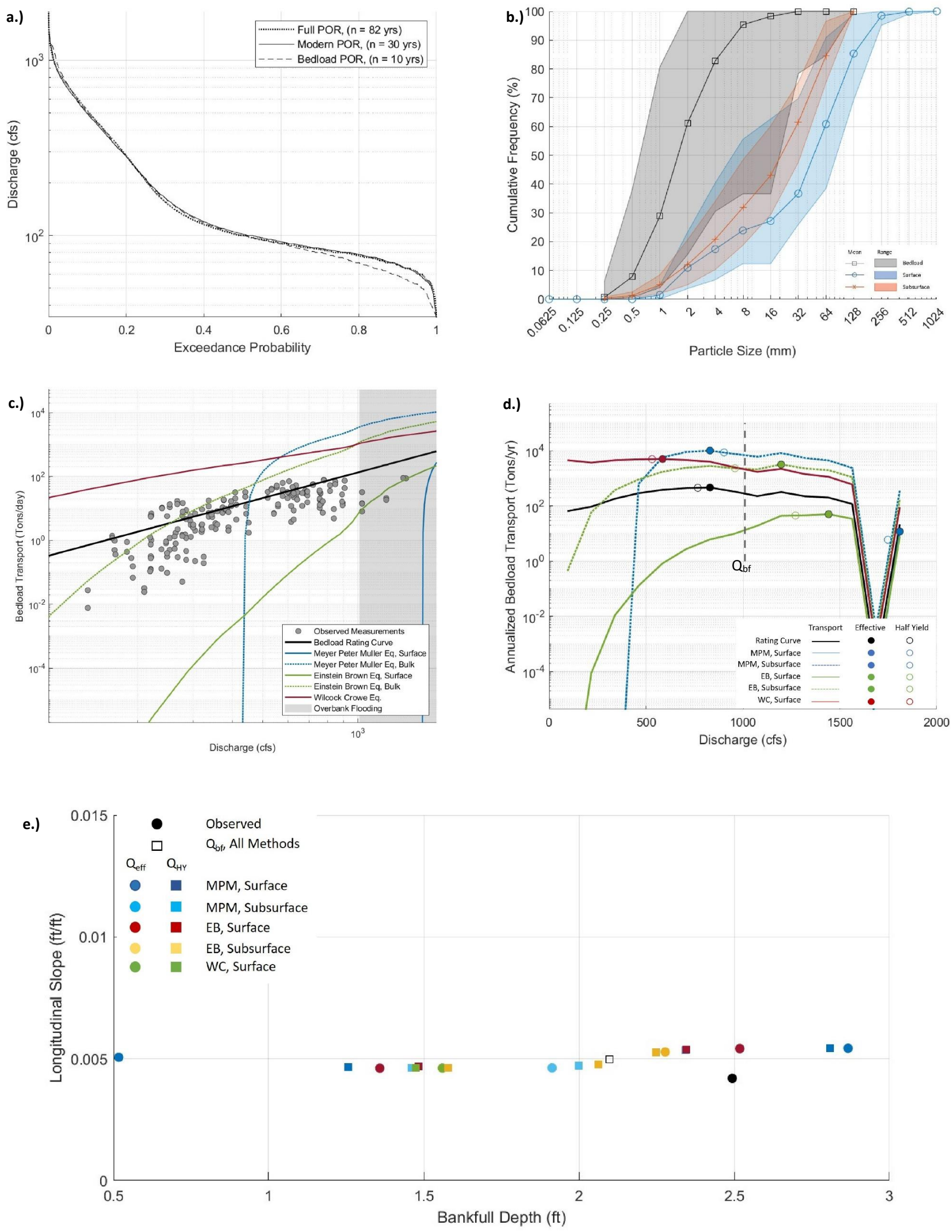

Figure A.22: *Results of analytical channel design procedure for Valley Creek, ID showing a.) flow duration curve for full gage history and modern period of record used in analysis, b.) observed sediment and bedload gradations, c.) observed and calculated sediment rating curves, d.) calculated effective and half-yield discharges, and e.) calculated stable geometries compared to observed bankfull geometry.*

APPENDIX B

REGRESSION BETWEEN SITE OBSERVATIONS AND METHOD ERROR

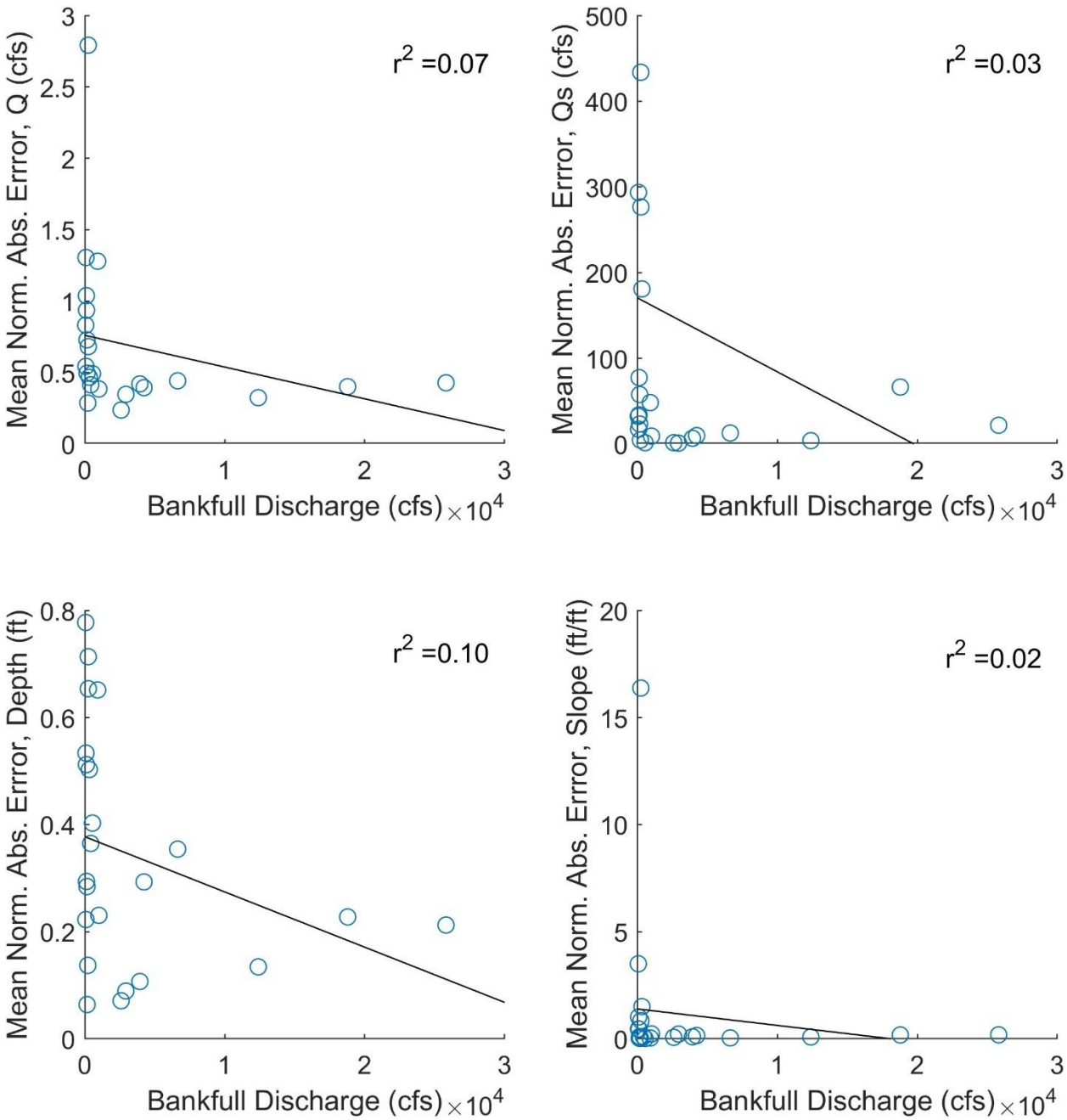

Figure B.1: *Linear regression between bankfull discharge and mean normalized absolute error in a.) design discharge, b.) design sediment load, c.) stable depth, and d.) stable slope.*

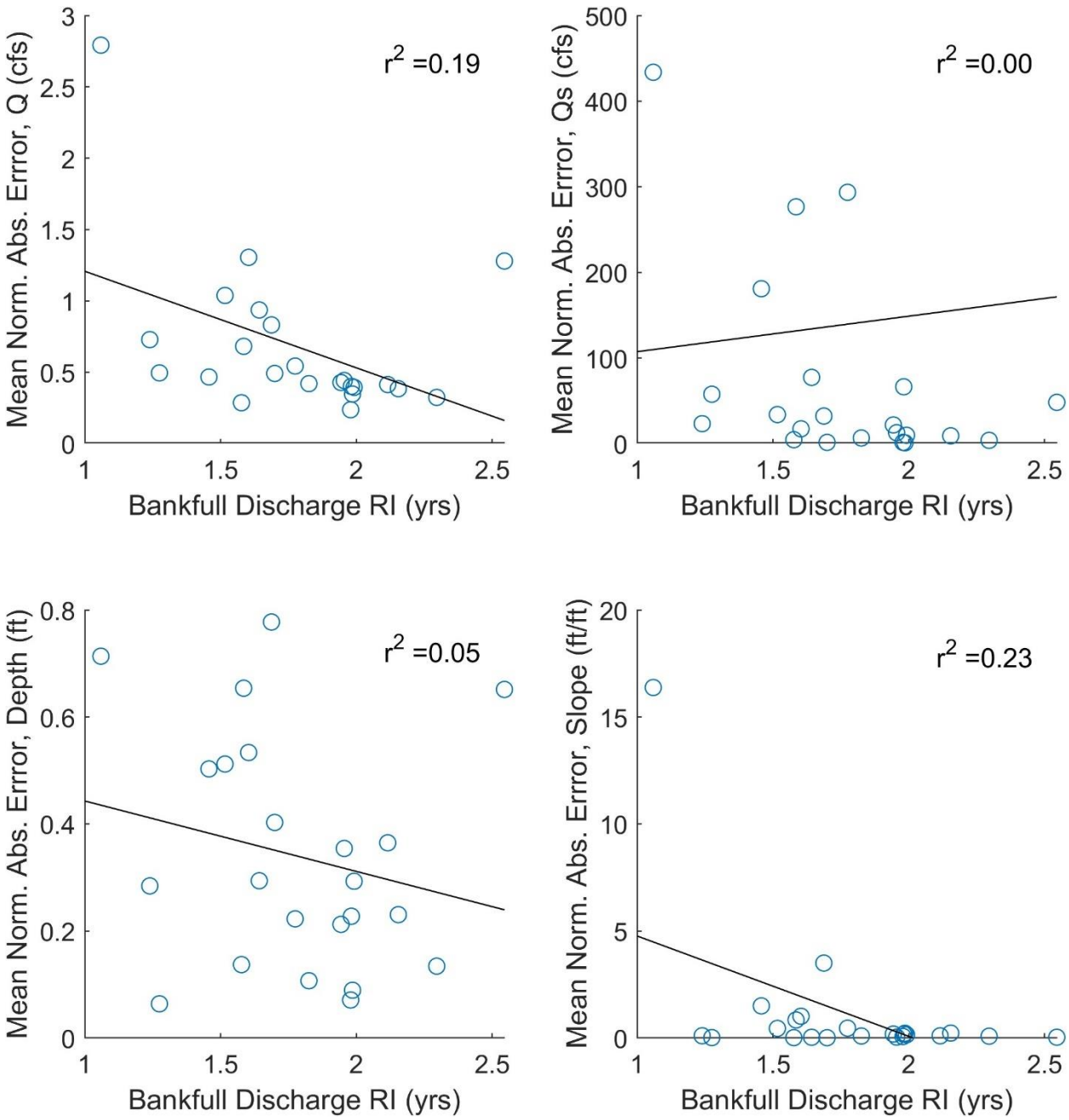

Figure B.2: *Linear regression between bankfull discharge recurrence interval (RI) and mean normalized absolute error in a.) design discharge, b.) design sediment load, c.) stable depth, and d.) stable slope.*

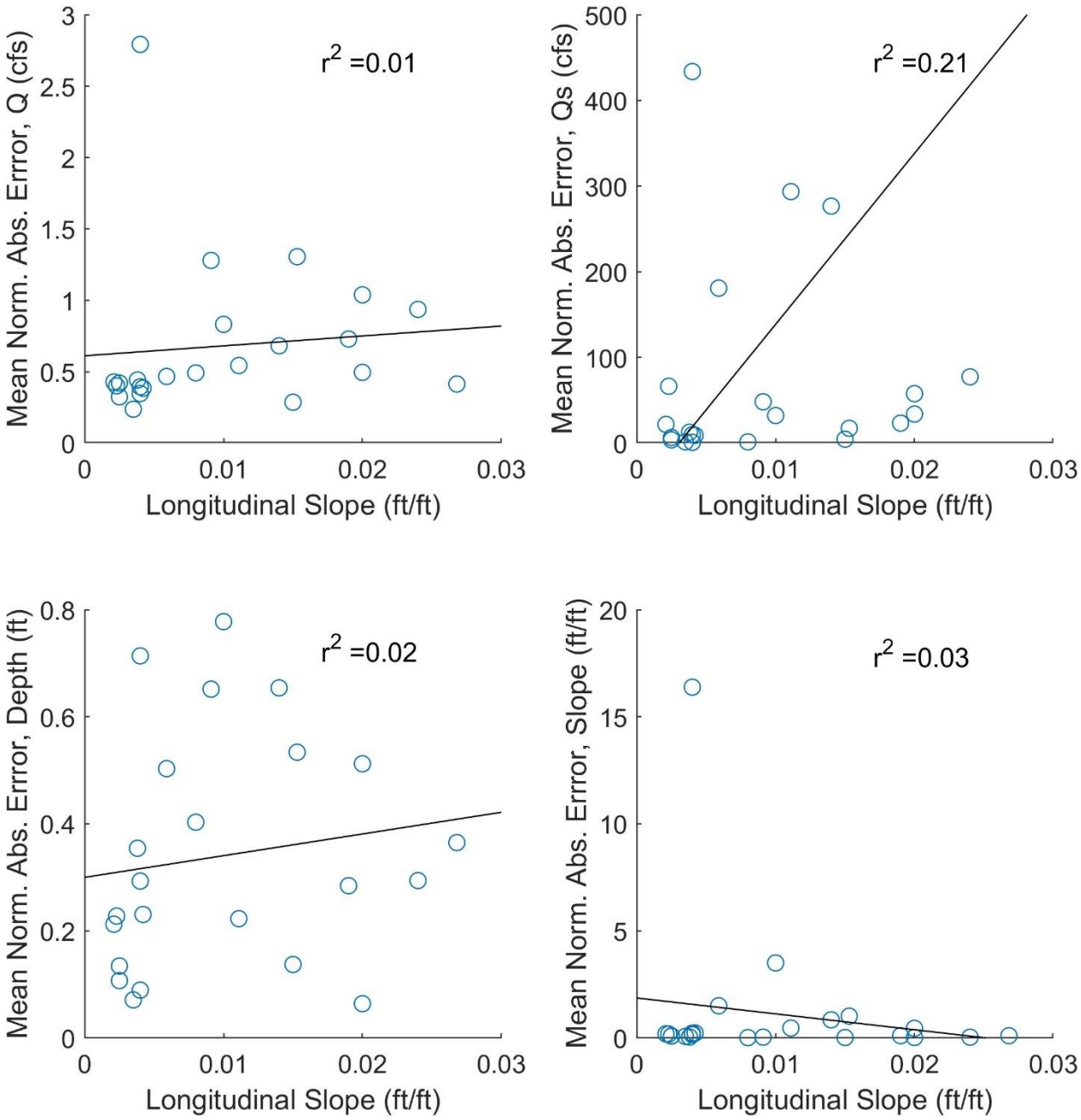

Figure B.3: *Linear regression between longitudinal channel slope and mean normalized absolute error in a.) design discharge, b.) design sediment load, c.) stable depth, and d.) stable slope.*

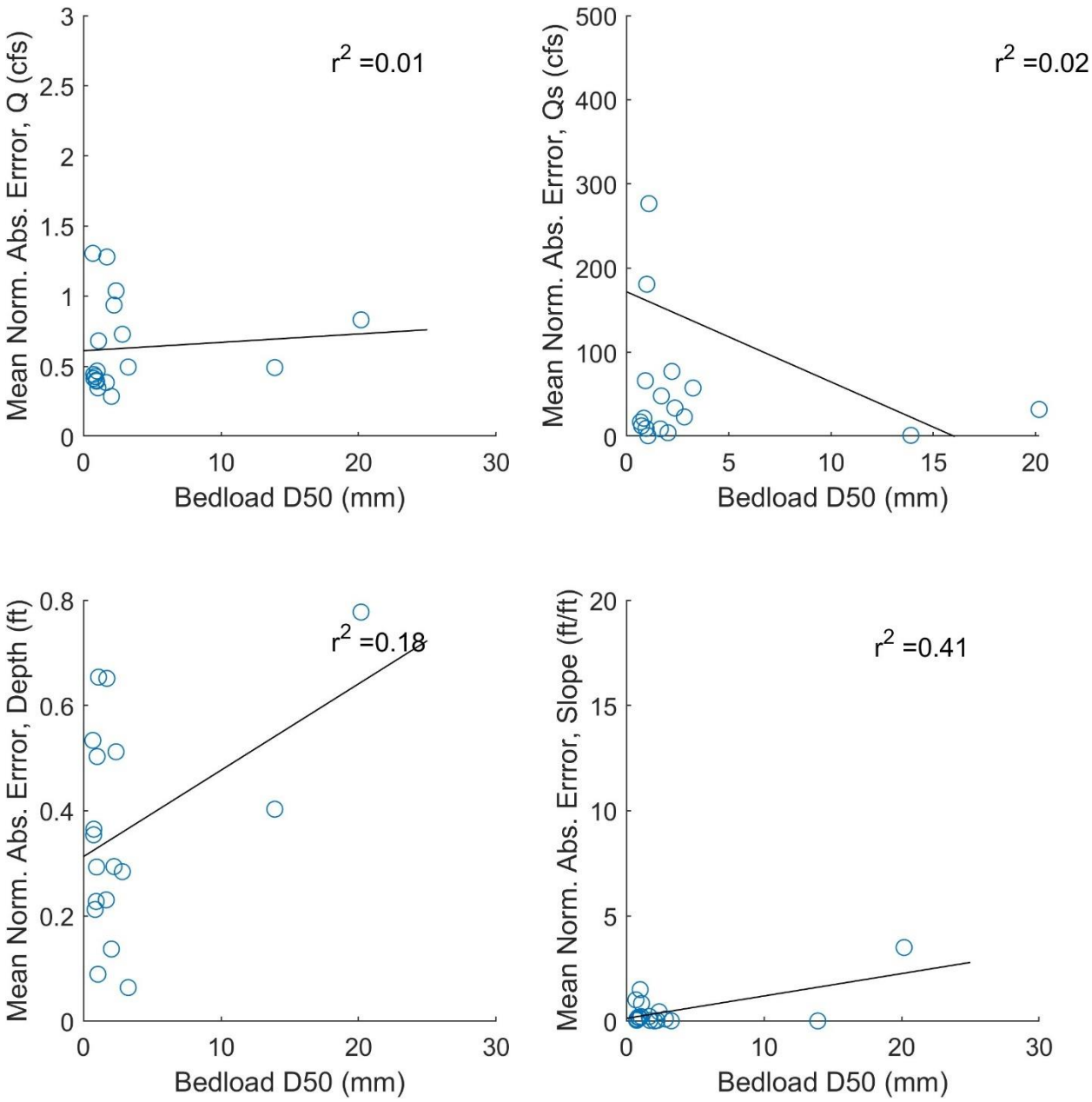

Figure B.4: *Linear regression between bedload D_{50} and mean normalized absolute error in a.) design discharge, b.) design sediment load, c.) stable depth, and d.) stable slope.*

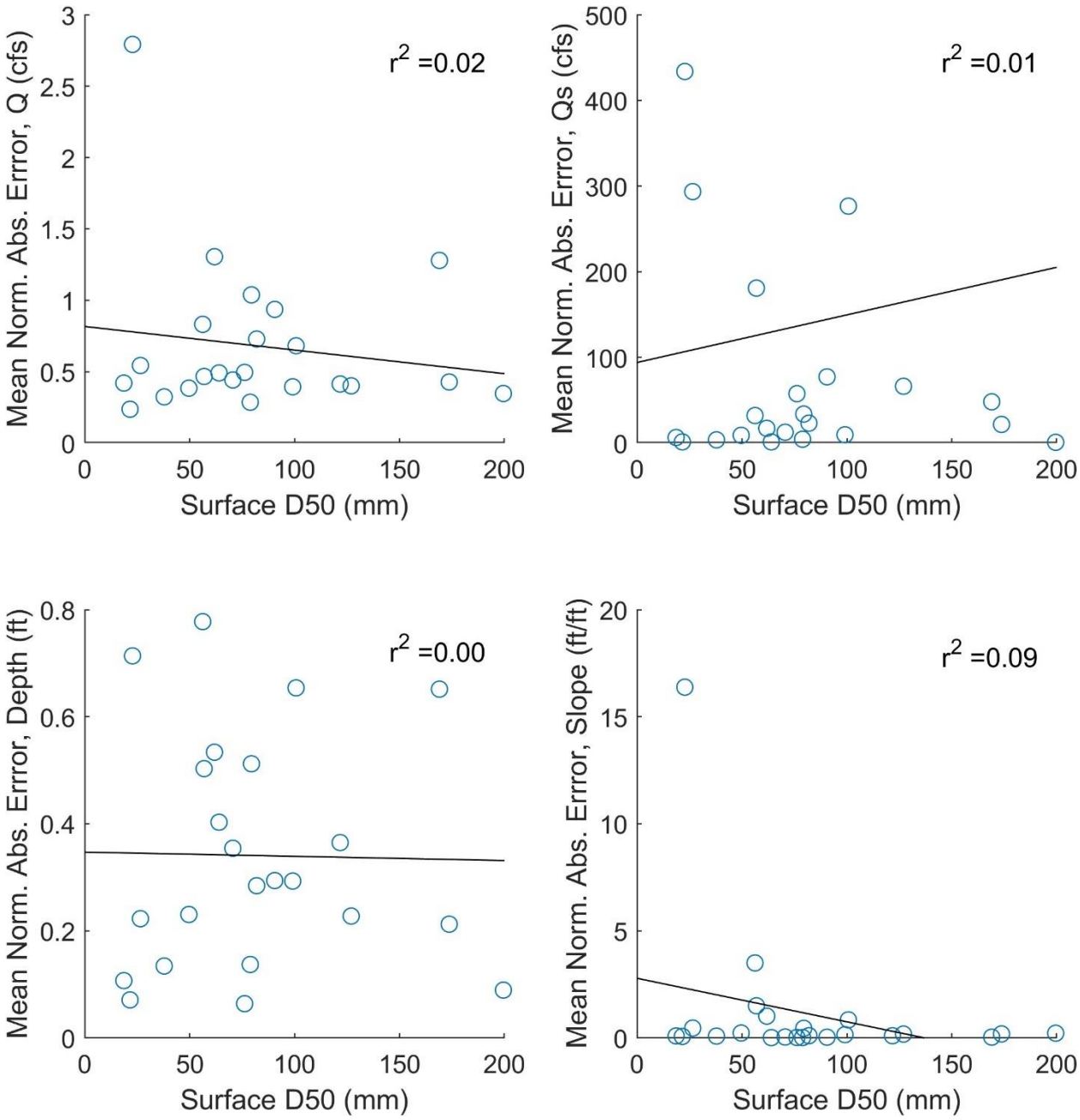

Figure B.5: *Linear regression between surface D_{50} and mean normalized absolute error in a.) design discharge, b.) design sediment load, c.) stable depth, and d.) stable slope.*

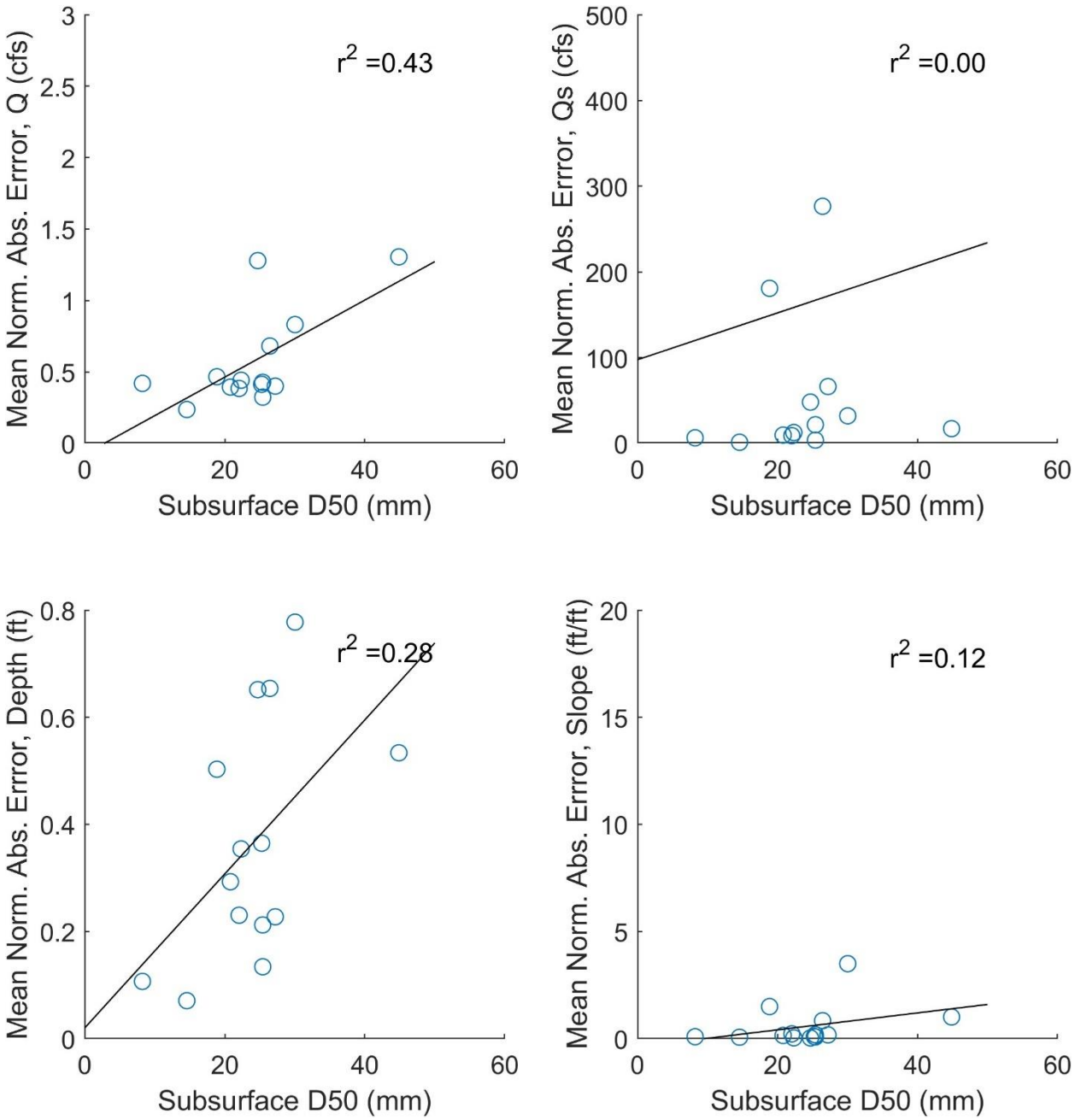

Figure B.6: *Linear regression between subsurface D_{50} and mean normalized absolute error in a.) design discharge, b.) design sediment load, c.) stable depth, and d.) stable slope.*

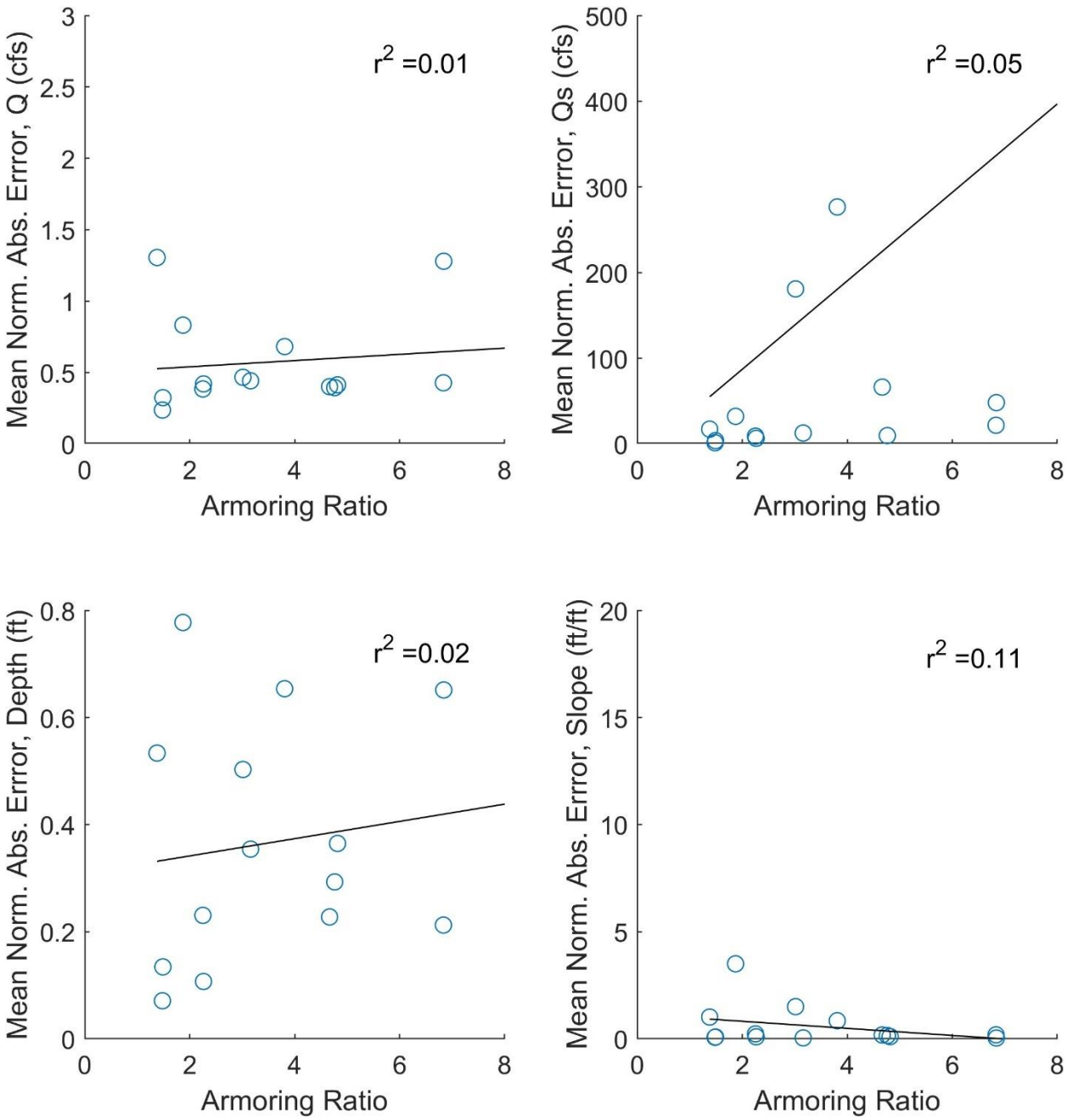

Figure B.7: *Linear regression between armoring ratio and mean normalized absolute error in a.) design discharge, b.) design sediment load, c.) stable depth, and d.) stable slope.*

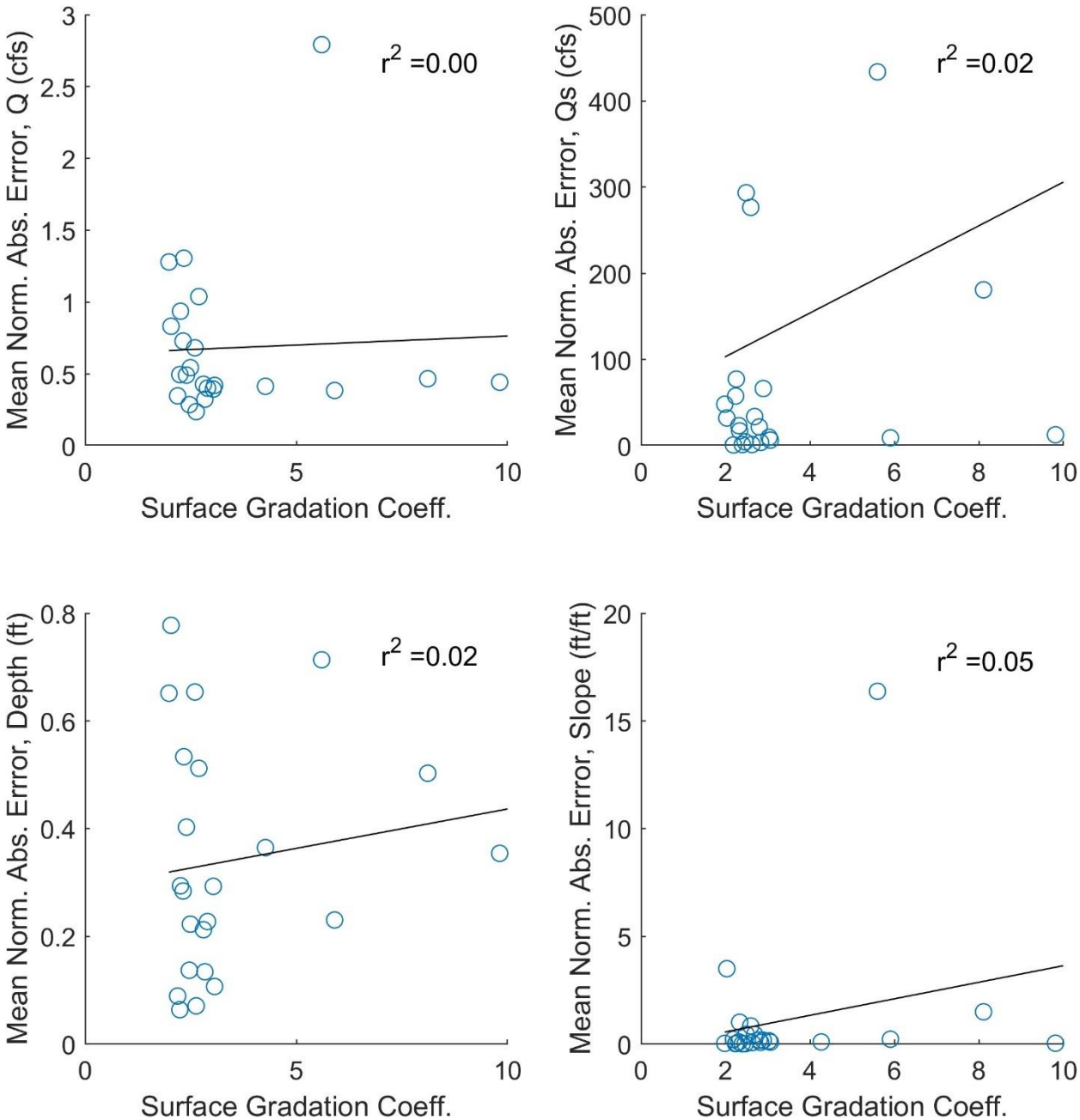

Figure B.8: *Linear regression between surface particle gradation coefficient and mean normalized absolute error in a.) design discharge, b.) design sediment load, c.) stable depth, and d.) stable slope.*

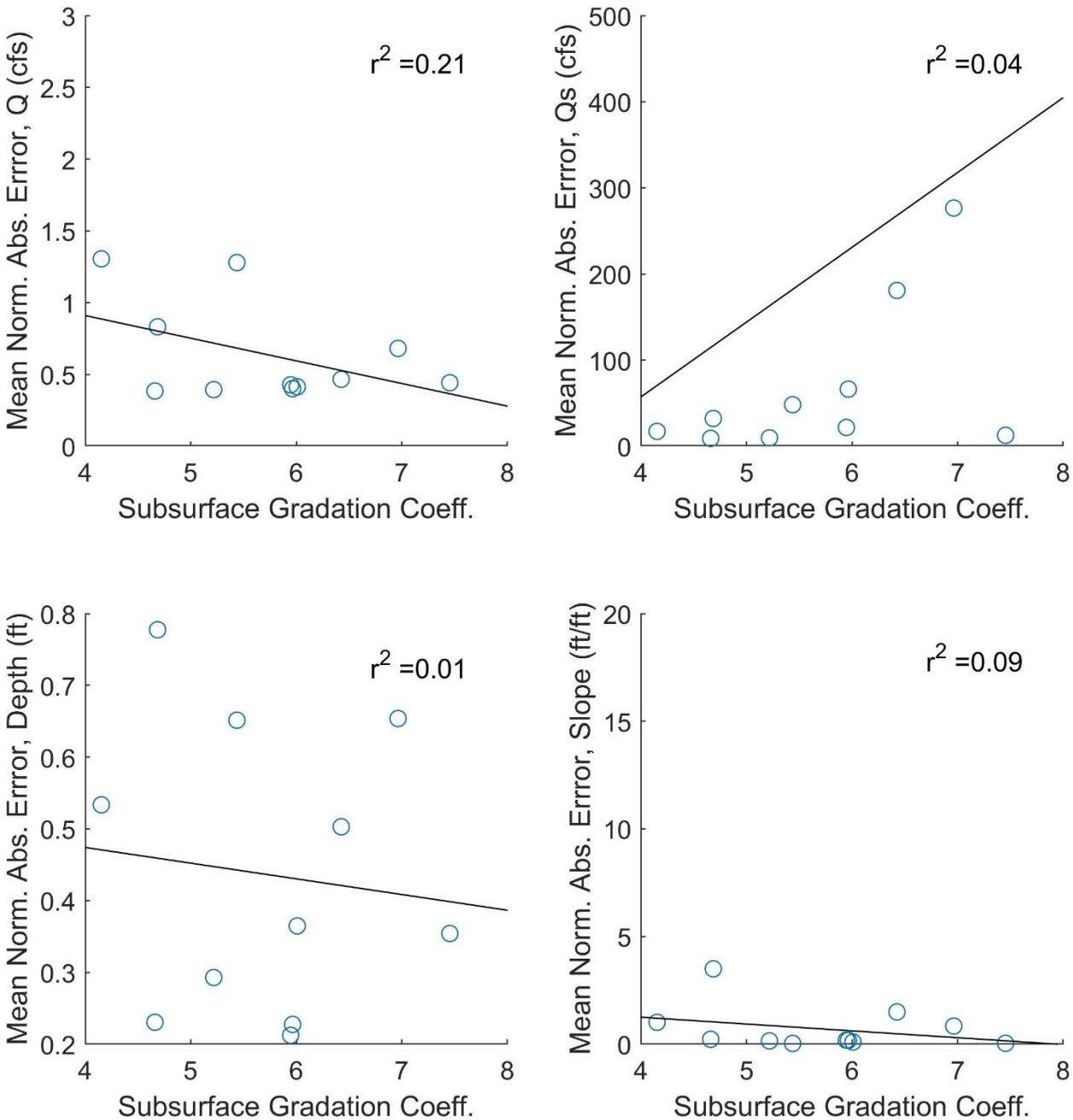

Figure B.9: *Linear regression between subsurface particle gradation coefficient and mean normalized absolute error in a.) design discharge, b.) design sediment load, c.) stable depth, and d.) stable slope.*